ION TRANSPORT IN CONDUCTING POLYMERS

GUANGCHUN LI

INFORMATION TO USERS

This manuscript has been reproduced from the microfilm master. UMI films the text directly from the original or copy submitted. Thus, some thesis and dissertation copies are in typewriter face, while others may be from any type of computer printer.

The quality of this reproduction is dependent upon the quality of the copy submitted. Broken or indistinct print, colored or poor quality illustrations and photographs, print bleedthrough, substandard margins, and improper alignment can adversely affect reproduction.

In the unlikely event that the author did not send UMI a complete manuscript and there are missing pages, these will be noted. Also, if unauthorized copyright material had to be removed, a note will indicate the deletion.

Oversize materials (e.g., maps, drawings, charts) are reproduced by sectioning the original, beginning at the upper left-hand corner and continuing from left to right in equal sections with small overlaps.

Photographs included in the original manuscript have been reproduced xerographically in this copy. Higher quality 6" x 9" black and white photographic prints are available for any photographs or illustrations appearing in this copy for an additional charge. Contact UMI directly to order.

Bell & Howell Information and Learning
300 North Zeeb Road, Ann Arbor, MI 48106-1346 USA
800-521-0600

Ion Transport in Conducting Polymers

by

Guangchun Li

A thesis submitted to the School of Graduate Studies

in partial fulfilment of the requirements for the degree of Master of Science

Department of Chemistry

Memorial University of Newfoundland

St. John's, Newfoundland

Canada

August 1999

ABSTRACT

The ion transport properties and electrochemistry of chemically prepared polypyrrole/poly(styrene-4-sulfonate), poly(3,4-ethylenedioxythiophene)/poly(styrene-4-sulfonate), and electrochemically prepared poly(3,4-ethylenedioxythiophene)/poly(styrene-4-sulfonate) composites have been investigated by cyclic voltammetry and impedance spectroscopy in a variety of electrolyte solutions. These polymers exhibited facile electrochemistry, fast ion transport, and good electrochemical stability. The chemically prepared polymers are approximately ten times more porous than their electrochemically prepared counterparts, and therefore have ionic conductivities that are higher by a similar factor and show less potential dependence. The ionic conductivities of these polymers are strongly dependent on the concentrations and conductivities of the electrolyte solution used. At low electrolyte concentrations, the ionic conductivities of these polymers also show some potential dependence. It is concluded that these polymers consist of permselective polymer phases containing incorporated counter- ions and pores containing the electrolyte solution. The incorporated ions account for the dependence of ionic conductivity on the applied potential and the polymer's intrinsic ionic conductivity, while the electrolyte solution in the pores explains the strong dependence of ionic conductivity on the solution concentration and conductivity. In high concentration electrolyte solutions, ion transport is dominated by electrolyte in the pores, while at low electrolyte concentrations, incorporated ions in the polymer phases become significant.

ACKNOWLEDGMENTS

I wish to express my greatest thanks to my supervisor, Dr. Peter G. Pickup, for his guidance, encouragement, help, kindness, and generosity.

I also would like to express my appreciation to other members of our research group for their help and kindness.

Many thanks to Lisa Lee of the Department of Biology for her guidance in X-Ray emission analysis and scanning electron microscopy.

Finally, I am grateful to the School of Graduate Studies, Chemistry Department, and NSERC for financial support.

CONTENTS

ABSTRACT i

ACKNOWLEDGMENTS ii

LIST OF TABLES vii

LIST OF FIGURES viii

LIST OF ABBREVIATIONS AND SYMBOLS USED xi

Chapter 1 INTRODUCTION TO CONDUCTING POLYMERS 1

1.1 BACKGROUND 1

1.2 ION TRANSPORT IN CONDUCTING POLYMERS 4

1.2.1 Overview 4

1.2.2 Influencing Factors 6

1.2.2.1 Structure and Morphology 6

1.2.2.2 The Size of the Dopant 7

1.2.2.3 The Applied Potential 8

1.2.2.4 Concentration of the External Electrolyte 8

1.2.2.5 Mobility of Ions 9

1.2.2.6 Solvent 9

1.2.3 Techniques 10

1.3 ELECTROCHEMISTRY OF CONDUCTING POLYMERS 10

1.3.1 Overview 10

1.3.2 Theory 11

1.4 OVEROXIDATION 12

1.4.1 Definition 12

1.4.2 Mechanism of Overoxidation 13

1.5 SYNTHESIS OF CONDUCTING POLYMERS BY OXIDATIVE POLYMERIZATION 15

1.5.1 Overview 15

1.5.2 Chemical Methods 15
1.5.3 Electrochemical Methods 16
1.6 APPLICATIONS 19
1.7 OBJECTIVES OF THIS WORK 20

Chapter 2 EXPERIMENTAL 25

2.1 ELECTROCHEMISTRY 25
2.2 IONIC CONDUCTIVITY MEASUREMENTS 25
2.2.1 Principle 25
2.2.2 Instruments 28
2.3 ELECTRONIC CONDUCTIVITY MEASUREMENTS 28
2.4 X-RAY EMISSION ANALYSIS 29
2.5 SCANNING ELECTRON MICROSCOPY 29
2.6 FOURIER TRANSFORM INFRARED SPECTROSCOPY 29
2.7 CHEMICALS AND MATERIALS 30

Chapter 3 CELL AND REFERENCE ELECTRODE DEVELOPMENT 32

3.1 INTRODUCTION 32
3.2 CELL DESIGN 33
3.3 PREPARATION OF THE PT/PPY/PSS REFERENCE ELECTRODE 33
3.4 RESULTS 35
3.5 CONCLUSIONS 35

Chapter 4 ION TRANSPORT IN CHEMICALLY PREPARED POLYPYRROLE /POLY(STYRENE-4-SULFONATE) COMPOSITES 42

4.1 INTRODUCTION 42
4.2 RESULTS AND DISCUSSION 44

4.2.1 Preparation of PPY/PSS Composites 44
4.2.2 Composition of PPY/PSS Composites 44
4.2.3 Electronic Conductivities of the Dry PPY/PSS Powders 45
4.2.4 Conductivities of the Electrolyte Solutions 47
4.2.5 Morphologies of PPY/PSS Samples 48
4.2.6 Cyclic Voltammetry 48
4.2.7 Impedance Spectroscopy 57
4.2.8 Use of Nafion Membranes as the Electrolyte 66
4.2.9 Morphology of Chemically Prepared PPY/PSS Layers 67
4.3 CONCLUSIONS 71

Chapter 5 ION TRANSPORT IN POLY(3,4-ETHYLENEDIOXYTHIOPHENE) /POLY(STYRENE-4-SULFONATE) COMPOSITES 73

5.1 INTRODUCTION 73
5.2 RESULTS AND DISCUSSION 75
5.2.1 Preparation of PEDOT/PSS Composites 75
5.2.1.1 Electrochemical Methods 75
5.2.1.2 Chemical Methods 75
5.2.2 Composition of the e-PEDOT/PSS Composites 77
5.2.3 Thickness of e-PEDOT/PSS Films and c-PEDOT/PSS Layers 77
5.2.4 Morphologies of e-PEDOT/PSS Films and c-PEDOT/PSS Powders 81
5.2.5 Cyclic Voltammetry 81
5.2.6 Impedance Spectroscopy 82
5.3 CONCLUSIONS 94

Chapter 6 COMPARISON BETWEEN PEDOT/PSS AND PPY/PSS SYSTEMS AND GENERAL CONCLUSIONS 96

6.1 INTRODUCTION 96
6.2 COMPOSITION 96

6.3 ELECTROCHEMISTRY 97
6.4 ION TRANSPORT 97
6.5 MORPHOLOGY 98
6.6 CONCLUSIONS 98

LIST OF TABLES

Table 3.1. Potentials (mV) of a PPY/PSS coated Pt wire (vs. SSCE) in various 0.5 M aqueous electrolyte solutions.

Table 3.2. Potentials (mV) of a PPY/PSS coated Pt wire (vs. SSCE) after 1 hour in various solutions of H_2SO_4(aq).

Table 4.1. Elemental analysis of a PPY/PSS composite.

Table 4.2. Ionic conductivities (mS cm^{-1}) of the aqueous electrolyte solutions employed.

Table 4.3. Voltammetric charges and specific capacitances in 0.5 M H_2SO_4(aq) for various loadings of PPY/PSS on a 0.2 cm^2 electrode.

Table 4.4. Specific Faradaic pseudocapacitances (F g^{-1}) at +0.1 V (vs Pt/PPY/PSS), from 10 mV s^{-1} cyclic voltammetry and impedance spectroscopy on 2.5 mg cm^{-2} PPY/PSS layers in various 0.5 M aqueous electrolyte solutions.

Table 4.5. Ionic conductivities (mS cm^{-1}) of PPY/PSS layers in various electrolyte solutions at 0.1 V vs Pt/PPY/PSS.

Table 5.1. Ionic conductivities (mS cm^{-1}) of c-PEDOT/PSS layers in various aqueous electrolyte solutions at 0 V vs Pt/PPY/PSS.

Table 5.2. Ionic conductivities (mS cm^{-1}) of e-PEDOT/PSS films in various aqueous electrolyte solutions at 0.2 V vs SSCE.

Table 5.3. Ionic resistances and conductivities of e-PEDOT/PSS films in 0.5 M $LiClO_4$(aq) as a function of film thickness at 0.2 V vs SSCE.

LIST OF FIGURES

Figure 1.1. The most widely studied conducting polymers.

Figure 1.2. Schematic diagram of charge and discharge of a conducting polymer: a. small anions incorporated; b. immobilized large anions incorporated.

Figure 1.3. Proposed mechanism of overoxidation of polypyrrole in the presence of water.

Figure 1.4. The most widely accepted mechanism for the electropolymerization of pyrrole.

Figure 2.1. a. Finite transmission-line equivalent circuit for a polymer coated electrode: b. corresponding complex plane impedance plot.

Figure 3.1. Schematic diagram of the sandwich-type cell. WE: working electrode; RE: reference electrode; CE: counter electrode.

Figure 3.2. Cyclic voltammograms (10 mV s^{-1}) of a chemically prepared PPY/PSS layer (2.5 mg cm^{-2}) in contact with 0.05 M $LiClO_4$ + CH_3CN.

Figure 3.3. Complex plane impedance plots for a chemically prepared PPY/PSS layer (2.5 mg cm^{-2}) in contact with $LiClO_4$ (aq) of various concentrations at 0.1 V vs Pt/PPY/PSS.

Figure 3.4. Cyclic voltammograms of (10 mV s^{-1}) of a chemically prepared PPY/PSS layer (2.5 mg cm^{-2}) containing 5% polyvinylferrocene in contact with 0.5 M LiCl(aq).

Figure 4.1. EDX spectrum of a c-PPY/PSS sample.

Figure 4.2. SEM micrographs of (a) c-PPY/PSS and (b) e-PPY/PSS.

Figure 4.3. Cyclic voltammograms (20 mV s^{-1}) of a c-PPY/PSS layer (2.5 mg cm^{-2}) in contact with 0.1 M H_2SO_4(aq).

Figure 4.4. Cyclic voltammograms (10, 20, 30, and 40 mV s^{-1}) of a c-PPY/PSS layer (2.5 mg cm^{-2}) in contact with 0.5 M Et_4NCl(aq).

Figure 4.5. Cyclic voltammograms (10 mV s^{-1}) of a c-PPY/PSS layer (2.5 mg cm^{-2}) in contact with 0.5 M $LiClO_4$ + CH_3CN.

Figure 4.6. Anodic currents (at 0 V vs Pt/PPY/PSS) of a c-PPY/PSS layer (2.5 mg cm^{-2}) in 0.5 M Et_4NCl(aq) at scan rates of 10, 20, 30, and 40 mV s^{-1}.

Figure 4.7. Cyclic voltammograms (10, 20, 30, and 40 mV s^{-1}) of a c-PPY/PSS layer (7.5 mg cm^{-2}) in contact with 0.5 M H_2SO_4(aq).

Figure 4.8. Complex plane impedance plots at 0.1 V vs Pt/PPY/PSS for a c-PPY/PSS layer (2.5 mg cm^{-2}) in contact with H_2SO_4(aq) of various concentrations.

Figure 4.9. Ionic conductivity of c-PPY/PSS at 0.1 V vs Pt/PPY/PSS as a function of electrolyte concentration in H_2SO_4(aq). Data for two different electrodes are shown (■ and ♦), together with a linear least squares fit of all of the data. R^2 is ca. 0.99.

Figure 4.10. Ionic conductivity of c-PPY/PSS at 0.1 V vs Pt/PPY/PSS in aqueous solutions of H_2SO_4 (•), HCl (♦), $LiClO_4$ (○), LiCl (◇), $NaClO_4$ (■), NaCl (□), Na_2SO_4 (△), and Et_4NCl (▲), as a function of electrolyte conductivity. R^2 is ca. 0.91.

Figure 4.11. Ionic conductivities of c-PPY/PSS layer (2.5 mg cm^{-2}) in (△) $LiClO_4$+CH_3CN and (x) $LiClO_4$(aq) of various concentrations at 0.1 V vs Pt/PPY/PSS.

Figure 4.12. Complex plane impedance plots for a c-PPY/PSS layer (2.5 mg cm^{-2}) at various applied potentials vs Pt/PPY/PSS in contact with 0.5 M H_2SO_4(aq).

Figure 4.13. Complex plane impedance plots for a c-PPY/PSS layer (2.5 mg cm^{-2}) in pressure contact with a hydrated Nafion membrane (potentials vs Pt/PPY/PSS).

Figure 4.14. EDX spectra of c-PPY/PSS: a. after 12 hours in contact with a Nafion membrane, b. without exposure to a Nafion membrane.

Figure 4.15. A morphological model for PPY/PSS layers and films, and the corresponding equivalent circuit.

Figure 5.1. Cyclic voltammetric synthesis (100 mV s^{-1}) of PEDOT/PSS from a saturated aqueous EDOT solution containing 0.1M PSS using a 0.071 cm^2 glassy carbon electrode.

Figure 5.2. Cyclic voltammogram (40 mV s^{-1}) of a e-PEDOT/PSS film (19 μm) in 0.5 M KNO_3(aq).

Figure 5.3. EDX spectra of a e-PEDOT/PSS film (19 μm) reduced in 0.5 M KNO_3(aq) at (a) 0 V and (b) -1 V vs SSCE.

Figure 5.4. SEM micrographs of (a) e-PEDOT/PSS and (b) c-PEDOT/PSS.

Figure 5.5. Cyclic voltammograms (20 mV s^{-1}) of (a) a c-PEDOT/PSS layer (5 mg cm^{-2}) and (b) a e-PEDOT/PSS film (14 μm) in contact with 0.5 M Et_4NCl(aq).

Figure 5.6. Anodic currents (at 0 V) of (a) a e-PEDOT/PSS film (14 μm) and (b) a c-PEDOT/PSS layer (2.5 mg cm^{-2}) as a function of scan rate in 0.5 M Et_4NCl(aq).

Figure 5.7. Complex plane impedance plots for (a) a c-PEDOT/PSS layer (2.5 mg cm^{-2}) at 0 V vs Pt/PPY/PSS and (b) a e-PEDOT/PSS film (14 μm) at 0.2 V vs SSCE in contact with LiCl (aq).

Figure 5.8. Ionic conductivity of c-PEDOT/PSS at 0 V vs Pt/PPY/PSS in aqueous solutions of H_2SO_4 (•), HCl (♦), $LiClO_4$ (○), LiCl (◇), $NaClO_4$ (■), NaCl (□), Na_2SO_4 (△), and Et_4NCl (▲), as a function of electrolyte conductivity. R^2 is ca. 0.89.

Figure 5.9. Ionic conductivity of e-PEDOT/PSS at 0.2 V vs SSCE in aqueous solutions of H_2SO_4 (•), HCl (♦), $LiClO_4$ (○), LiCl (◇), $NaClO_4$ (■), NaCl (□), Na_2SO_4 (△), and Et_4NCl (▲), as a function of electrolyte conductivity. R^2 is ca. 0.92.

Figure 5.10. Complex plane impedance plots for (a) a c-PEDOT/PSS layer (2.5 mg cm^{-2}) and (b) a e-PEDOT/PSS film (14 μm) in contact with 0.5 M $LiClO_4$(aq) at various applied potentials vs Pt/PPY/PSS for the c-PEDOT/PSS and SSCE for the e-PEDOT/PSS.

Figure 5.11. Ionic conductivities of (a) c-PEDOT/PSS and (b) e-PEDOT/PSS in 0.05 M H_2SO_4(aq) as a funtion of applied potential.

LIST OF ABBREVIATIONS AND SYMBOLS USED

Symbol	Meaning	Unit
A	electrode area	cm^2
A^-	small anion	
appl.	applied	
aq	aqueous	
c	chemically prepared	
C^+	cation	
CFP	carbon fibre paper	
C_i	concentration of mobile ions	mole L^{-1}
conc.	concentration of electrolyte solution	mole L^{-1}
d	film thickness	μm
e	electrochemically prepared	
EDX	energy dispersive x-ray emission spectroscopy	
EDOT	3,4-ethylenedioxythiophene	
E_{eq}	equilibrium potential of working electrode	mV
E_{appl}	applied potential	mV
FTIR	Fourier transform infrared spectroscopy	
F	Faraday constant	96500 C mol^{-1}
I	current	mA
L^-	fixed large anion	
PANI	polyaniline	
PEDOT	poly(3,4-ethylenedioxythiophene)	
PPY	polypyrrole	
PPY/PSS	polypyrrole/poly(styrene-4-sulfonate)	
PSS	poly(styrene-4-sulfonate)	
PTFE	poly(tetrafluoroethylene)	
PTh	polythiophene	

Pt/PPY/PSS	PPY/PSS-coated fine Pt wire reference electrode	
R_e	electronic resistance	ohm
R_i	ionic resistance	ohm
R_{sol}	solution resistance	ohm
SEM	scanning electron microscopy	
sol.	solution	
SSCE	saturated sodium chloride calomel electrode	
U_i	mobility of ions	$m^2 (sV)^{-1}$
V	voltage	mV
$\|Z\|$	absolute charge of mobile ions	
Z'	real impedance	ohm
Z''	imaginary impedance	ohm
η	overpotential	mV
σ_{ion}	ionic conductivity	mS cm^{-1}
σ_{sol}	solution conductivity	mS cm^{-1}
σ_{KCl}	solution conductivity of 1M KCl(aq)	mS cm^{-1}

Chapter 1 INTRODUCTION TO CONDUCTING POLYMERS

1.1 BACKGROUND

Conducting polymers, which can be defined as polymers containing long chains of alternating single and double bonds [1], have attracted tremendous interest in physics, chemistry and materials science [2-4]. Possessing the advantages of high conductivity, light weight, flexibility, and plasticity, they have huge potential for applications in electronic devices and the batteries to power them [2, 5, 6]. Although polyacetylene was the first reported conducting polymer [2], it has poor chemical and electrochemical stability [7], so currently the most studied conducting polymers (Fig. 1.1) are polypyrrole, polythiophene, polyaniline and their substituted analogues.

Conducting polymers are generally poor intrinsic conductors. In the neutral state, their conductivities are usually low. When they are doped (oxidized or reduced), their conductivities increase tremendously, in some cases by more than 10 orders of magnitude [1]. Their conductivities are strongly dependent on the doping level, which is controlled by the applied potential. Maximum electronic conductivities are typically 1 - 1000 S cm^{-1}.

The electronic conduction mechanism of conducting polymers is generally explained by band theory [1,8,9]. When a conducting polymer is in its undoped state, the valence band is filled and the conduction band is empty. The band gap is generally too large for electrons to be thermally excited from the valence band to the conduction band, so the conductivity is very low. When the polymer is oxidized, mobile holes (polarons) are

PPY

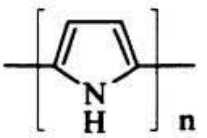

PTh

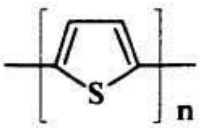

PANI

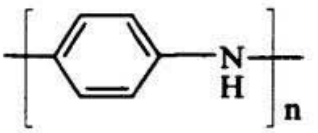

Figure 1.1. The most widely studied conducting polymers.

produced in the valence band. When the polymer is reduced, mobile electrons are added to the conduction band. At the same time, oxidation or reduction changes the polymer's structure and creates various mid-gap states. The creation of mid-gap states facilitates the excitation of charge carriers (polarons or electrons) and enhances the conductivity of the polymer greatly.

The dependence of the electronic conductivity of a conducting polymer on applied potential means that its conductivity can be easily manipulated either electrochemically or with chemical redox species. This really is a unique advantage of conducting polymers over other conducting materials.

When a conducting polymer is prepared by either chemical or electrochemical oxidation, generally there are positive charges distributed along the polymer chains. Counter-ions from solution are incorporated into the polymer matrix to electrostatically neutralize the charged polymer as Equation 1.1 shows.

$$\{m_x^+\}_n + nA^-(sol.) = \{m_x^+\}_n nA^- \qquad (1.1)$$

where x is the number of monomer units that share one positive charge, and A^- is the incorporated anion. The resulting polymer is therefore actually a salt of the polymer and the incorporated counter-ions. The incorporated counter-ions have a major influence on the properties and applications of the polymers. This is another unique characteristic of conducting polymers.

1.2 ION TRANSPORT IN CONDUCTING POLYMERS

1.2.1 Overview

Conducting polymers can be viewed as mixed-conductors, because they are both electronic and ionic conductors [10]. The electrochemistry and many of the applications of conducting polymers involve both electron and ion transport. In general, electron transport is much faster than ion transport in conducting polymers, so ion transport is often the rate determining step [11]. Therefore, fully understanding ion transport in conducting polymers is crucial to understanding their electrochemistry and optimizing many of their applications.

As Figure 1.2 illustrates, the charge and discharge of a conducting polymer involves counter-ions, anions or cations, moving into, or out of, the polymer to maintain electroneutrality. When a polymer prepared in the presence of a small anion is discharged and recharged, the anions move out of, and back into, the polymer and the polymer is permselective to anions. This process can be expressed by the following equation:

$$\{m_x^+\}_n nA^- + ne \underset{\text{charge}}{\overset{\text{discharge}}{\rightleftharpoons}} \{m_x\}_n + nA^-(\text{sol.}) \qquad (1.2)$$

When a conducting polymer is prepared in a solution of a large anion, such as a polyanion, the large anion is incorporated into the polymer to compensate the positive charge and becomes trapped because of structural hindrance. When such a polymer is reduced and reoxidized, cations (C^+) must move into, and out of, the polymer to neutralize the immobilized anions. Thus, conducting polymer/large anion composites are generally

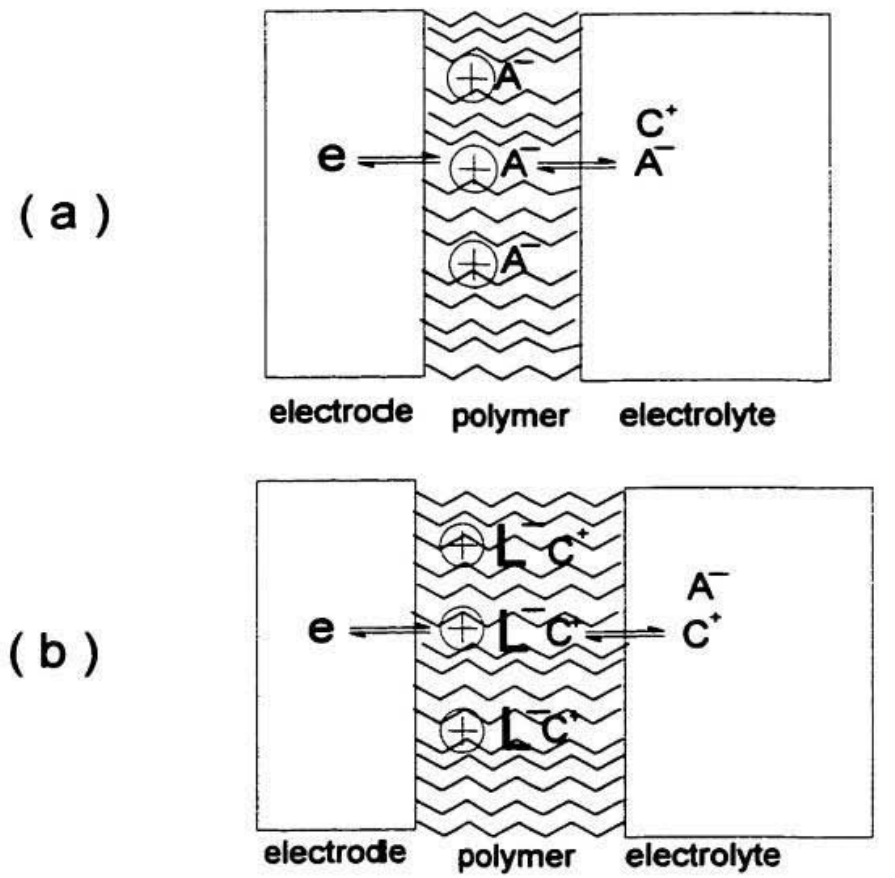

Figure 1.2. Schematic diagram of charge and discharge of a conducting polymer: a. small anions incorporated; b. immobilized large anions incorporated.

permselective to cations [12-16] as expressed in Equation 1.3.

$$(\{m_x^+\}_n nA^-_{large}) + nC^+(sol.) + ne \underset{charge}{\overset{discharge}{\rightleftharpoons}} (\{m_x\}_n nA^-_{large})nC^+ \qquad (1.3)$$

Because cations are generally smaller than anions and therefore have higher mobilities, ion transport in polymers with immobilized large anions is usually much faster than that in polymers doped with small anions. Fast ion transport can enhance the electrochemical process and result in high energy density when conducting polymers are used as energy storage materials [17].

1.2.2 Influencing Factors

The study of ion transport in conducting polymers is still the subject of controversy and uncertainty, because a large number of factors influences the results [18].

1.2.2.1 Structure and Morphology

Ion transport in a conducting polymer with a loose fibrous structure is much faster than with a compact, low porosity structure. Naoi and Shougi [19] electropolymerized pyrrole in the presence of a surfactant to produce highly microporous polypyrrole films with greatly enhanced ion transport rates. They also obtained a very rough, porous polypyrrole with similarly improved ion transport properties through the use of etched tubular channels as a template.

The study of ion transport in conducting polymers can provide valuable insight into

their structures. Ren and Pickup [20] studied the structure of electropolymerized polypyrrole films by impedance measurements of ionic conductivity and proposed a morphological model. These authors concluded that electropolymerized polypyrrole consists of permselective polymer aggregates which enclose pores, and that there is poor interconnectivity between pores. They also found that chemically prepared polypyrrole /poly(styrene-4-sulfonate) powders have proton conductivities as high as 0.03 S cm^{-1} when pressed as ca. 50 μm thick layers on Nafion membranes, which is 100 times higher than the proton conductivity of an electropolymerized polypyrrole/poly(styrene-4-sulfonate) film immersed in 1 M H_2SO_4 (aq) [12]. This big difference in ionic conductivity may have been due to the different morphologies of the samples.

1.2.2.2 The Size of the Dopant

The size of the dopant (counterion) greatly influences the rate of ion transport in a conducting polymer. Naoi and Shouji [19] have studied electropolymerized polypyrrole with various dopants and have found that there are different ion exchange properties depending on the size of the dopant as Equations 1.2 and 1.3 illustrate. Ren and Pickup [21] have found that the ionic conductivity of electropolymerized polypyrrole doped with a large anion (poly(styrene-4-sulfonate)) is significantly higher than that of polypyrrole doped with a small anion (perchlorate). This result can be explained by the higher mobility of cations over anions and a strong H-bonding interaction between ClO_4^- and oxidized polypyrrole.

1.2.2.3 The Applied Potential

Ion transport in conducting polymers can depend greatly on the applied potential, which controls the degree of oxidation of the polymer. When a conducting polymer is oxidized (high potential), anions move into the polymer if it is doped with a small anion or cations move out of the polymer if it is doped with a large immobilized anion. In contrast, when a conducting polymer is reduced (low potential), anions move out of the polymer or cations move in. Burgmayer and Murray [22,23] have shown that oxidized polypyrrole doped with Cl^- exhibits a much higher anion conductivity than cation conductivity, while the neutral polymer was almost impermeable to ions. They concluded that the cationic form of the polymer was permselective to anions. Ren and Pickup [21] have found that the ionic conductivity of electropolymerized polypyrrole doped with perchlorate increases with increasing applied potential, while the ionic conductivity of polypyrrole doped with poly(styrene-4-sulfonate) decreases. When pyrrole was electropolymerized in the presence of the anion surfactant dodecylsulfate, the resulting polypyrrole films were found to behave as dual mode ion exchangers (i.e., anion or cation exchangers) simply by controlling the applied potential [19].

1.2.2.4 Concentration of the External Electrolyte

The specific conductivity σ_{ion} of the considered phase is given by:

$$\sigma_{ion} = \sum F |Z_i| U_i C_i \quad (1.4)$$

where U_i is the physical mobility, C_i is the concentration, and $|Z_i|$ is the absolute charge of

each mobile ion [24]. As Equation 1.4 indicates, increasing the concentration of mobile ions will increase ionic conductivity, and experimental results are consistent with this expectation. Ren and Pickup [20] have found that the ionic conductivities of polypyrrole perchlorate and polypyrrole/poly(styrene-4-sulfonate) increase almost linearly with increasing electrolyte concentration in aqueous $NaClO_4$, NaCl and HCl. Our results are also consistent with Equation 1.4.

1.2.2.5 Mobility of Ions

Equation 1.4 indicates that ionic conductivities are also proportional to the mobilities of the ions in the polymer layer. Because H^+ has a much higher mobility than Na^+, the ionic conductivity of polypyrrole/polystyrene-4-sulfonate in HCl(aq) is far higher than in NaCl(aq) or $NaClO_4$(aq) of the same concentration [20].

1.2.2.6 Solvent

The electrochemistry of conducting polymers can be heavily influenced by the solvent [25,26]. Two main types of effect have been discussed. Firstly, different solvents have different swelling effects on the polymer. Secondly, solvent molecules may accompany doping ions moving into, or out of, the conducting polymer during charge and discharge. The use of laser beam deflection at the polymer-electrolyte interface and the electrochemical quartz crystal microbalance to monitor mass change has demonstrated that there is often solvent transport during the charge and discharge of conducting polymers [27-

29].

1.2.3 Techniques

The two most important and powerful techniques that have been widely used to investigate ion transport in conducting polymers are impedance spectroscopy and the electrochemical quartz crystal microbalance. The former can be used to measure the ionic conductivity of a conducting polymer film at various conditions, such as at different applied potentials or in different electrolyte solutions of different concentration [1,30]. The latter can directly monitor nanogram-order mass change during electrochemical processes and provide identification of mobile ions and neutral species [15,31].

X-Ray photoelectron spectroscopy and X-Ray emission spectroscopy are also useful techniques for determining which ions have been incorporated into a conducting polymer film under various conditions [21,32].

1.3 ELECTROCHEMISTRY OF CONDUCTING POLYMERS

1.3.1 Overview

The electrochemistry of conducting polymers involves both electron and ion transport as indicated in Equations 1.2 and 1.3. The electrochemical properties of conducting polymers are generally studied by cyclic voltammetry. Cyclic voltammograms of conducting polymers are significantly different from those of redox conducting polymers

for which accepted theory is available [1]. When a conducting polymer is oxidized (p-doping), there is a broad, flat plateau anodic current as the potential increases beyond the anodic peak, rather than a rapid decay to close to zero as observed for redox polymers. A large broad capacitance-like wave is also seen on the reverse scan. The large peak separation, which is virtually independent of the scan speed, and the asymmetric capacitance-like waves indicate that the redox processes of conducting polymers do not obey the Nernst equation [1].

The cyclic voltammograms of conducting polymers heavily depend on the nature of the polymer, the synthetic conditions, and the solution in which cyclic voltammetry is performed [1]. For example, Liu and coworkers [33] have found that there is a big difference in cyclic voltammograms of electrochemically prepared polyaniline and chemically prepared polyaniline. Electrochemically prepared films have two sets of redox peaks, while only one set of redox peaks is observed with the chemically prepared material.

Because the redox process of a conducting polymer also involves ion transport, ions moving into, and out of, the conducting polymers during charge and discharge also influence the cyclic voltammograms [34,35]. For example, Lefebvre and coworkers [36] found that cyclic voltammograms of poly(3,4-ethylenedioxthiophene)/poly(styrene-4-sulfonate) show some differences when the cation or solvent are varied.

1.3.2 Theory

The theory of the redox processes of conducting polymers is still a topic of debate

[1,37]. Several explanations have been proposed to model the large variety of capacitance-like cyclic voltammograms of conducting polymers. One of the most accepted is that there are different segments in a conducting polymer, and therefore there are multiple redox sites with different redox potentials. Another theory explains the capacitance-like voltammograms of conducting polymers by the interaction between oxidized chains and structural relaxation [1,37].

1.4 OVEROXIDATION

1.4.1 Definition

Qi [38] studied the cyclic voltammetry of poly(3-methylthiophene) over different potential ranges. When the potential is kept below 1.0 V, a reversible redox process is observed. The cyclic voltammograms change very little on successive scans. However, when the anodic potential is increased to 2.0 V, a large irreversible redox process is produced. The anodic and cathodic currents decrease tremendously with successive cycling. This degradation of electroactivity and conductivity of a conducting polymer at high anodic potential is termed overoxidation. Because overoxidation causes a conducting polymer to lose its electroactivity and conductivity, even becoming an insulator, much attention must be paid to the applied potential range during synthesis and study of a conducting polymer.

1.4.2 Mechanism of Overoxidation

The mechanism of overoxidation is poorly understood. Pud [39] assumed that overoxidation proceeded simultaneously by two mechanisms: crosslinking and a nucleophilic process. The crosslinking process accounts for the conductivity decrease, and the brittleness and insolubility of overoxidized conducting polymers. On the other hand, the nucleophilic mechanism explains changes in the polymer's functional groups and composition, as well as the effects of solvent and supporting electrolyte. In weakly nucleophilic media, overoxidation by crosslinking will prevail, while in highly nucleophilic media, the nucleophilic mechanism will dominate.

Water is the most common nucleophilic agent in overoxidation of conducting polymers [40,41]. Figure 1.3 [42] illustrates a proposed mechanism for the overoxidation of polypyrrole in the presence of water. After reaction with water, the polymer loses its conjugation and its conductivity is extremely decreased.

Although overoxidation is one of the main drawbacks of conducting polymers, it also has some useful applications. These interesting applications include directly modifying a polymer and producing a new substituted conducting polymer in the presence of a suitable nucleophile [1,39].

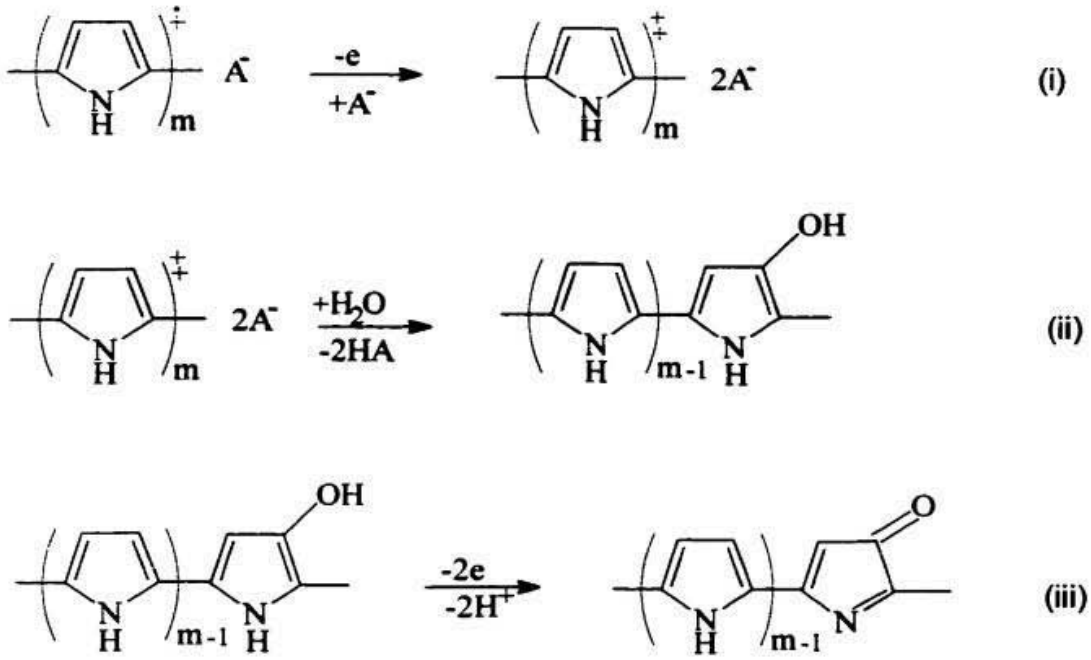

Figure 1.3. **Proposed mechanism of overoxidation of polypyrrole in the presence of water [42].**

1.5 SYNTHESIS OF CONDUCTING POLYMERS BY OXIDATIVE POLYMERIZATION

1.5.1 Overview

Except for polyacetylene, the most widely studied conducting polymers can be polymerized both by chemical and electrochemical oxidation of monomers in appropriate solutions [43]. Generally, the synthetic conditions are not harsh, but the properties of the resulting conducting polymer, such as conductivity, ion transport properties, morphology and solubility, are strongly dependant on the synthetic conditions [1,44], which makes reproducibility problematic. On the other hand, the heavy dependence of the properties of conducting polymers on synthetic conditions provides the means to improve and manipulate the properties of conducting polymers by choosing appropriate synthetic conditions, such as solvent, electrolyte, oxidizing agent, potential and current. Conducting polymers synthesized in different electrolyte solutions incorporate different doping ions and therefore may have different properties, such as solubility, ion transport characteristics and processability.

1.5.2 Chemical Methods

The most widely studied conducting polymers, polypyrrole, polythiophene, polyaniline and their substituted analogues, have been chemically synthesized by using oxidizing agents in suitable solutions [45-50]. The most commonly used oxidizing agents

include Fe(III) salts, $(NH_4)_2S_2O_8$, KIO_3 and H_2O_2. The structural, chemical and physical properties of the resulting conducting polymers heavily depend on the properties of the oxidizing agent, the ratio of oxidizing agent to monomer, the solvent, the electrolyte and the temperature. Qi and Pickup [51] achieved size-control of polypyrrole particles by varying the ratio of oxidizing agent, Fe^{3+}, to monomer, pyrrole, in the presence of poly(styrene-4-sulfonate). They found that the higher the ratio (Fe^{3+} : pyrrole) the smaller the particle size. Liu and coworkers [33] enzymatically synthesized water-soluble, conducting polyaniline in the presence of poly(styrene-4-sulfonate) as a template. This novel method is simple and the synthetic conditions are mild. The solubility and processability of the polyaniline are greatly improved. According to these authors, the poly(styrene-4-sulfonate) serves three functions: first, to align preferentially the aniline monomers and promote a more ordered para-directed reaction; second, to provide counter-ions for doping of the synthesized polyaniline; and third, to maintain water-solubility for processing.

Chemical methods for the synthesis of conducting polymers have the advantages of low cost, speed, and freedom from the restrictions of electrodes. Chemical methods are well suited for mass production.

1.5.3 Electrochemical Methods

Most conducting polymers can also be conveniently synthesized by electrochemical methods [37,43]. These include potentiostatic, galvanostatic and potential-cycling techniques. Cyclic voltammetry is a simple and powerful technique to synthesize and study

electrochemically a conducting polymer. Cyclic voltammetry is very useful to determine if a monomer can be electrochemically polymerized under certain conditions. The indication of successful synthesis is that the anodic and cathodic currents increase with successive cycles. Galvanostatic polymerization, using constant anodic current, is the most commonly used way to synthesize conducting polymers. With this method, the thickness of the conducting polymer can be easily controlled by controlling the consumed charge. The commonly used electrode materials are platinum and carbon.

Compared with chemical methods, the advantages of electrochemical methods are the following:

(i) A highly electrochemically active and conductive polymer film can be easily produced on an electrode, which can be directly used as an electrode in a battery or as a sensor [52,53].

(ii) Film thickness, morphology and conductivity can be easily controlled by monitoring the applied potential and current.

(iii) They are cleaner than chemical methods because no oxidizing agents are used.

(iv) They provide an in situ way to investigate the polymerization process and the properties of the resulting conducting polymer.

The mechanism of electropolymerization is still debatable [1,37]. Experiments show that α-substituted pyrrole cannot be polymerized [54]. The most widely accepted mechanism for electropolymerization of pyrrole is shown in Figure 1.4 [55,56].

i . radical formation

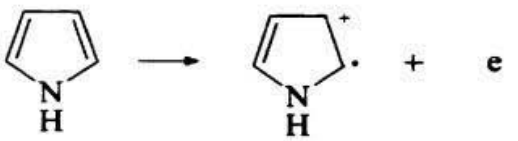

ii . coupling

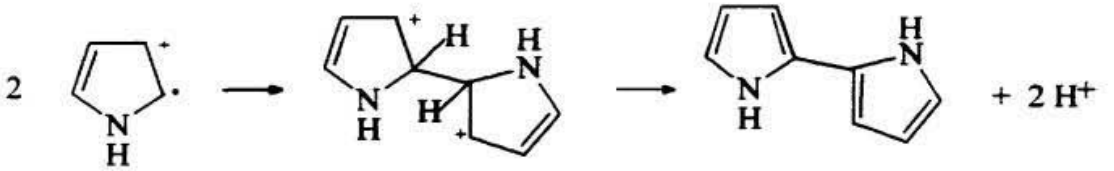

iii. propagation

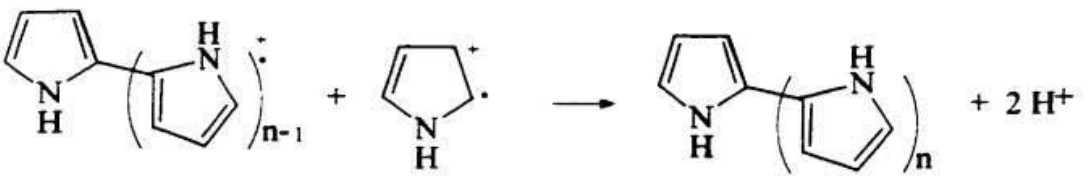

iv. doping

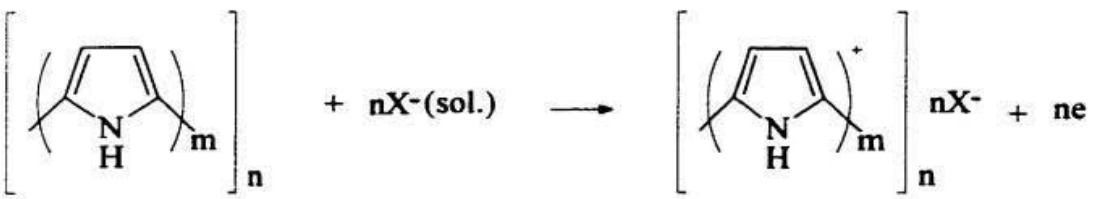

Figure 1.4. The most widely accepted mechanism for the electropolymerization of pyrrole [55,56].

1.6 APPLICATIONS

With the advantages of high electronic conductivity combined with flexibility and plasticity, the applications of conducting polymers have been the focus of intensive study in recent years [2,5,57]. The most widely studied application areas are in batteries [43,44], fuel cells [58,59], supercapacitors [60,61], sensors [62,63], electronic devices [64,65], and antistatic materials [66].

The most promising and widely studied applications of conducting polymers are as cathode materials in lithium batteries [6,15,43] as indicated by Equation 1.5, where cp^+ is the repeated polymer unit that carries one positive charge.

$$\{cp^+\}_n + n\,Li \underset{\text{charge}}{\overset{\text{discharge}}{\rightleftharpoons}} \{cp\}_n + n\,Li^+ \qquad (1.5)$$

Due to safety problems with lithium, intensive attention has been diverted to lithium-ion batteries, which have the advantages of high energy density, high cell voltage, good safety and are friendly to the environment [67,68]. In lithium-ion batteries, lithium intercalation materials are used as anodes, rather than lithium metal, so safety issues from the high reactivity of lithium are greatly alleviated. Other lithium intercalation materials are used as cathodes. Lithium ions move back and forth between the anode and cathode during charge and discharge.

The charge and discharge of a conducting polymer/polyanion composite involves cations moving into, and out of, the polymer matrix, making the conducting polymer/polyanion composite suitable as a cathode material in a lithium-ion battery.

Considering the advantages of conducting polymers, their use as cathode materials for portable lithium-ion batteries is promising and feasible.

1.7 OBJECTIVES OF THIS WORK

The ionic conductivities of packed layers of chemically prepared polypyrrole/poly(styrene-4-sulfonate) (PPY/PSS) are much higher than those of electrochemically prepared PPY/PSS films [21], but the reason is unclear. The main objective of this thesis work was therefore to try to understand why there is such a large difference in the ionic conductivities of these two materials, and also to provide further information about factors influencing ion transport in conducting polymers. The approach taken was to measure the ionic conductivities of various electrochemically and chemically prepared polymers under various conditions by impedance spectroscopy. The ions incorporated into the polymer films were determined by elemental analysis, X-Ray analysis and FTIR. The structure and morphologies of the polymers were determined by scanning electron microscopy. The combination of ionic conductivities, morphology, and analysis of doping ions provides a clear picture of ion transport in the conducting polymers studied.

References

1. Pickup, P.G. In *Modern Aspects of Electrochemistry*; Conway, B. E.; Bockris, J. O'M.; White, R. E., Eds.; Plenum: New York, in press.

2. Scotl, C. J. *Science* **1997**, 278, 2071.

3. Skotheim, T. A.; Elsenbaumer, R. L.; Reynolds, J. R., Eds. *Hanbook of Conducting Polymers*, 2nd Ed.; Marcel Dekker: New York, 1998.

4. Nalwa, H. S., Ed. *Handbook of Organic Conductive Molecules and Polymers*; Wiley: Chichester, UK, 1997; Vol. 2-4.

5. Miller, J. S. *Adv. Mater.* **1993**, 5, 587.

6. Scrosati, B. In *Handbook of Solid State Batteries & Capacitors*; Munshi, M. Z. A., Ed.; World Scientific: Singapore, 1995; Chapter 14.

7. Scrosati, B. *Prog. Solid State Chem.* **1988**, 18, 1.

8. Bredas, L.; Chance, R. R.; Silbey, R.; Nicolas, G.; Durand, P. *J. Chem. Phys.* **1982**, 76, 3673.

9. Bredas, L.; Chance, R. R.; Silbey, R.; Nicolas, G.; Durand, P. *J. Chem. Phys.* **1983**, 78, 5656.

10. Doblhofer, K. In *Electrochemistry of Novel Material*; Lipkowski, J.; Ross, P. N., Eds.; VCH Publishers, Inc.: New York, 1994; p142.

11. Scrosati, B. In *Handbook of Solid State Batteries & Capacitors*; Munshi, M. Z. A., Ed.; World Scientific: Singapore, 1995; p280.

12. Qi, Z.; Lefebvre, M. C.; Pickup, P. G. *J. Electroanal. Chem.* **1998**, 457, 9.

13. Shimizu, T.; Ohtani, A.; Iyoda, T.; Honda, K. *J. Electroanal. Chem.* **1987**, 224, 123.

14. Hyodo, K.; Omae, M. *Electrochim. Acta* **1990**, 35, 1245.

15. Baker, C. K.; Qiu, Y. J.; Reynolds, J. R. *J. Phys. Chem.* **1991**, 95, 4446.

16. Ehrenbeck, C.; Juttner, K. *Electrochim. Acta* **1996**, 41, 511.

17. Naoi, K.; Munshi, M. Z. A. In *Handbook of Solid State Batteries & Capacitors*; Munshi, M. Z. A., Ed.; World Scientific: Singapore, 1995; Chapter 17.

18. Armand, M.; Sanchez, J. Y.; Gaklhier, M.; Choquette, Y. In *Electrochemistry of Novel Material*; Lipkowski, J.; Ross, P. N., Eds.; VCH Publishers, Inc.: New York, 1994; p89.

19. Naoi, K.; Shouji, E. In *Handbook of Solid State Batteries & Capacitors*; Munshi, M. Z. A., Ed.; World Scientific: Singapore, 1995; Chapter 13.

20. Ren, X.; Pickup, P. G. *J. Electroanal. Chem.* **1995**, 396, 359.

21. Ren, X.; Pickup, P. G. *J. Phys. Chem.* **1993**, 97, 5356.

22. Burgmayer, P.; Murray, R. W. *J. Am. Chem. Soc.* **1982**, 104, 6139.

23. Burgmayer, P.; Murray, R. W. *J. Phys. Chem.* **1984**, 88, 2515.

24. Doblhofer, K. In *Electrochemistry of Novel Material*; Lipkowski, J.; Ross, P. N., Eds.; VCH Publishers, Inc.: New York, 1994; p159.

25. Duffitt, G. L.; Pickup, P. G. *J. Chem. Soc., Faraday. Trans.* **1992**, 88, 1417.

26. Zhang, W. B.; Dong, S. *J. Electrochem. Acta* **1993**, 38, 441.

27. Okabayashi, K.; Gato, F.; Abe, K.; Yoshida, T. *J. Electrochem. Soc.* **1989**, 136, 1986.

28. Hillman, A. R.; Swann, M. J.; Bruckensteir, S. *J. Phys. Chem.* **1991**, 95, 3271.

29. Bose, C. S. C.; Basak, S.; Rajeshwar, K. *J. Phys. Chem.* **1992**, 96, 9899.

30. Ren, X.; Pickup, P. G. *J. Chem. Soc., Faraday. Trans.* **1993**, 89, 321.

31. Buttry, D. A.; Ward, M. D. *Chem. Rev.* **1992**, 92, 1355.

32. Mirrezaei, S. R.; Munro, H. S.; Parter, D. *Synth. Met.* **1988**, 26, 169.

33. Liu, W.; Kumar, J.; Tripathy, S.; Senecal, K. J.; Samuelson, L. *J. Am. Chem. Soc.*

1999, 121, 71.

34. Warren, L. F.; Anderson, D. P. *J. Electrochem. Soc.* **1987**, 134, 101.

35. Kupila, E. L.; Lukkari, J.; Kankare, J. *Synth. Met.* **1995**, 74, 207.

36. Lefebvre, M. C.; Qi, Z.; Rana, D.; Pickup, P. G. *Chem. Mater.* **1999**, 11, 262.

37. Heinze, J. In *Topic in Current Chemistry*; Springer-Verlag: Berlin, 1990; Vol. 152.

38. Qi, Z. *M. Sc. Thesis*, Memorial University of Newfounland, 1992.

39. Pud, A. A. *Synth. Met.* **1994**, 66, 1.

40. Novak, P.; Rasch, B.; Vielstich, W. *J. Electrochem. Soc.* **1991**, 138, 3300.

41. Qi, Z.; Pickup, P. G. *Anal. Chem.* **1993**, 65, 696.

42. Beck, F.; Braun, P.; Oberst, M.; Bunsenges, B. *Phys. Chem.* **1987**, 91, 967.

43. Vovak, P.; Muller, K.; Santhanam, K. S. V.; Haas, O. *Chem. Rev.* **1997**, 97, 207.

44. Tsutsumi, H.; Yamashita, S.; Oishi, T. *J. Appl. Electrochem.* **1997**, 27, 477.

45. Mermilliod, N.; Tanguy, T.; Petiot, F. *J. Electrochem. Soc.* **1986**, 133, 1073.

46. Bjorklund, R.; Liedberg, B. *Chem, Commun.* **1986**, 1293.

47. Yamamoto, T.; Zama, M.; Yamamoto, A. *Chem. Lett.* **1985**, No. 5, 563.

48. Chen, S. A.; Kung, H. P.; Tasi, C. C.; Hou, C. S. *Synth. Met.* **1993**, 55, 582.

49. Armes, S. P.; Miller, J. F. *Synth. Met.* **1988**, 22, 385.

50. Pron, A.; Genoud, F.; Menardo, C.; Nechtschein, M. *Synth. Met.* **1988**, 24, 193.

51. Qi, Z.; Pickup, P. G. *Chem. Mater.* **1997**, 9, 2934.

52. Marchesiello, M.; Genies, E. *J. Electroanal. Chem.* **1993**, 358, 35.

53. Yamato, H.; Ohwa, M.; Wernet, W. *J. Electroanal. Chem.* **1995**, 377, 163.

54. Diaz, A. F.; Martinez, A.; Kanazawa, K. K.; Salmon, M. *J. Electroanal. Chem.* **1980**, 130, 181.

55. Naoi, K.; Osaka, T. *J. Electrochem. Soc.* **1987**, 134, 2479.

56. Andrieux, C. P.; Audebert, P.; Hapiat, P.; Suvent, J. M. *J. Phys. Chem.* **1991**, 95, 10158.

57. Macdiamid, A. G. *Synth. Met.* **1997**, 84, 27.

58. Coutanceau, C.; Elhourch, A.; Crouigneau, P.; Leger, J. M.; Lamy, C. *Electrochim. Acta* **1995**, 40, 2739.

59. Qi, Z.; Pickup, P. G. *Chem. Commun.* **1998**, 15.

60. Arbizzani, C.; Mastragostino, M.; Meneghello, L.; Paraventi, R. *Adv. Mater.* **1996**, 8, No. 4, 331.

61. Carlberg, G. C.; Inganas, O. *J. Electrochem. Soc.* **1997**, 144, No. 4, L61.

62. Yamato, H.; Ohwa, M.; Wernet, W. *J. Electroanal. Chem.* **1995**, 397, 163.

63. Hwang, B. J.; Yang, J.; Lin, C. *J. Electrochem. Soc.* **1999**, 146, 1231.

64. Chen, S. A.; Fang, Y. *Synth. Met.* **1993**, 60, 215.

65. Lenergan, M. C. *Science* **1997**, 278, 2103.

66. Wood, A. S. *Mod. Plast.* **1991**, August, 47.

67. Hossain, S. In *Handbook of Batteries*; Linden, D., Ed.; Magraw -Hill Inc.: New York, 1995; Chapter 36.

68. Appetecchi, G. B.; Scrosati, B. *Electrochim. Acta* **1998**, 43, 1105.

Chapter 2 EXPERIMENTAL

2.1 ELECTROCHEMISTRY

Electrochemical experiments were carried out either in conventional three-compartment glass cells at room temperature under nitrogen or in a sandwich-type cell developed in this work (see Ch.3). Platinum electrodes, glassy carbon electrodes (both sealed in glass) or a 0.2 cm^2 carbon fibre paper (CFP) disc, coated on one side with a polymer layer, were used as working electrodes. The reference electrode was a calomel electrode (SSCE) or a PPY/PSS-coated Pt wire electrode (Pt/PPY/PSS; see Section 3.3). The counter electrode was a Pt wire or a 1 cm^2 CFP electrode, coated with 5 mg of PPY/PSS or PEDOT/PSS. Potentials are quoted with respect to the SSCE reference electrode or the Pt/PPY/PSS reference electrode.

Voltammetric measurements were made with a HA-301 potentiostat/galvanostat (Hokuto Denko Ltd.) coupled with a HB-104 function generator (Hokuto Denko Ltd.) and a BBC SE 780 X-Y recorder.

2.2 IONIC CONDUCTIVITY MEASUREMENTS

2.2.1 Principle

The ionic conductivities of conducting polymers under various conditions were determined by impedance spectroscopy. The impedance responses of the polymers were

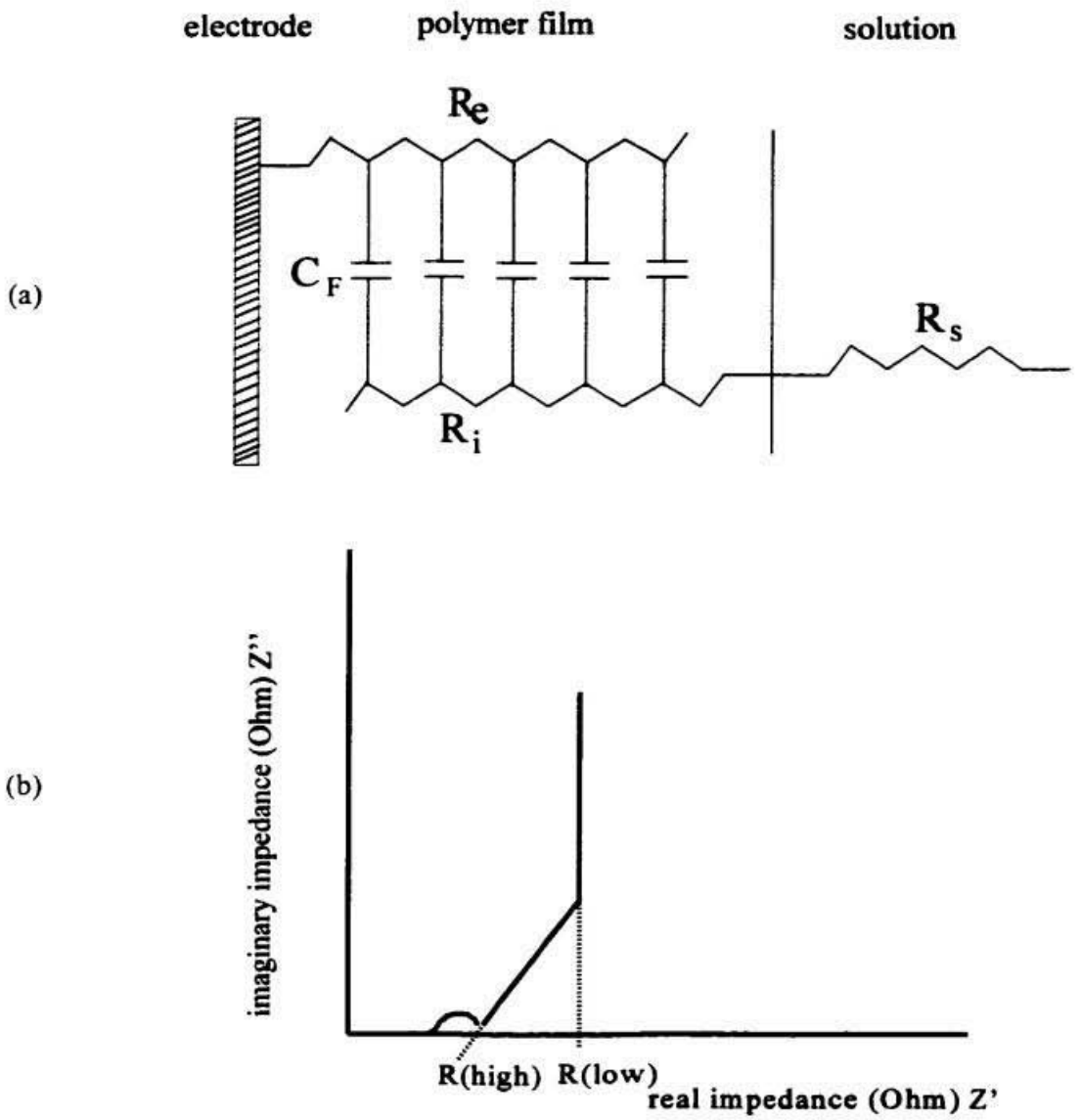

Figure 2.1. a. Finite transmission-line equivalent circuit for a polymer coated electrode; b. corresponding complex plane impedance plot.

modeled by a finite transmission-line equivalent circuit as shown in Figure 2.1(a) [1]. R_e is the electronic resistance of the polymer film, R_i is its ionic resistance, C_F is its Faradaic pseudo capacitance, and R_s is the uncompensated solution resistance. Figure 2.1(b) shows the corresponding complex plane impedance plot. The semicircle at high frequencies represents the charge transfer resistances at the interfaces, which are omitted from the equivalent circuit for clarity. The appearance of a large semicircle makes ionic resistance measurements uncertain. The Warburg-like region (45° slope) corresponds to both electron and ion transfer resistances within the film. The longer the Warburg-like region, the larger is the sum of the electron and ion transfer resistances. For precise ionic resistance measurements, the electronic resistance (R_e) should be negligible compared to the ionic resistance (R_i). At low frequencies, the vertical region (constant real impedance) corresponds to the total capacitance and resistance of the polymer film. Inhomogeneities and slow processes within the polymer film usually cause the low frequency part of the impedance plot to deviate from vertical (i.e., Z' continues to increase slightly even at the lowest accessible frequencies) [1-2].

The film's ionic resistance can be estimated from the complex plane impedance plot and is given by:

$$R_i = 3\,[R_{(low)} - R_{(high)}] \qquad (2.1)$$

where $R_{(high)}$ and $R_{(low)}$ are the real axis intercepts of the high frequency Warburg-like region and low frequency vertical region, respectively. The errors due to small deviations from ideality (i.e., Z' usually increases with decreasing frequencies in the low frequency region

where it should be constant, and the slope of the Warburg-like region deviates from 45°) is minor [2].

The ionic conductivity of the polymer film is calculated by the following equation:

$$\sigma_{ion} = d/R_i A \qquad (2.2)$$

where d is the thickness of the polymer film and A is the geometric area of the electrode [3].

2.2.2 Instruments

Impedance measurements were conducted with a perturbation amplitude of 5 mV RMS and scanned between 65 KHz and 0.1 Hz with a Solartron Frequency Response Analyzer (Model 1250) coupled to a Solartron Electrochemical Interface (Model 1268). All data were collected and analysed by a PC and commercial ZPLOT software (Scribner Associates Inc.).

2.3 ELECTRONIC CONDUCTIVITY MEASUREMENTS

The electronic conductivites of dry polymers were measured with a four-point probe in which the polymer was pressed in situ against four Pt wire contacts [4]. The thickness of the sample was measured with a linear vernier microscope (Griffin). The conductivity of the dry polymer is given by the following equation:

$$\sigma_e = I/4.27Vd \qquad (2.3)$$

where I is the applied current, V is the voltage drop and d is the thickness of the polymer

layer.

2.4 X-RAY EMISSION ANALYSIS

Energy dispersive X-Ray analysis is a simple, fast, and non-destructive technique which can be used to analyse the composition of conducting polymers treated under various conditions. It can easily be applied to thin films on electrodes. Generally, glassy carbon electrodes are preferred, because platinum electrodes produce large Pt peaks in EDX spectra.

X-Ray emission analysis was performed with a Tracor Northern 5500 Energy Dispersive X-Ray Analyzer coupled with a Hitachi-570 scanning electron microscope. All data were analysed with Tracor Northern Software (SQ), which has the merits of speed, convenience, and standardless analysis.

2.5 SCANNING ELECTRON MICROSCOPY

The structure and morphology of the polymers was observed with a Hitachi-570 scanning electron microscope. The electrochemically prepared polymers were directly observed on glassy carbon electrodes, while the chemically prepared samples were spread onto sample stubs as a paste with water and dried at room temperature.

2.6 FOURIER TRANSFORM INFRARED SPECTROSCOPY

FTIR is also a useful technique to analyse conducting polymers. For IR analysis, a

0.35 mg sample was ground with 150 mg KBr and pressed under vacuum into a transparent pellet of 1 cm diameter. Spectra were collected with a Mattson Polaris FTIR spectrometer at a nominal resolution of 4.0 cm^{-1}.

2.7 CHEMICALS AND MATERIALS

Pyrrole (PY, Aldrich) was purified by passing it through a dry SiO_2 (230–400 mesh) column and it was used immediately. 2,2-Dithiodianiline (DTDA, Aldrich), 3,4-ethylenedioxythiophene (EDOT, Bayer Trial Product), sodium poly(styrene-4-sulfonate) (PSS, Aldrich, M_w =70,000), poly(acrylic acid, sodium salt) (PAA, M_w = ca. 30,000, Aldrich, 40 wt %), and other chemicals were used as received. Poly(tetrafluoroethylene) (PTFE, 60% suspension in water, Dupont) was diluted to 15% with deionized water. Nafion 117 membranes (Dupont), carbon fibre paper (CFP, Toray TGPH90 +10%PTFE, Ballard), and other materials were used as received.

References

1. Pickup, P. G. In *Modern Aspects of Electrochemistry*; Conway, B. E.; Bockris, J. O'M.; White, R. E., Eds.; Plenum: New York, in press.

2. Ren, X.; Pickup, P. G. *J. Chem. Soc., Faraday. Trans.* **1993**, 89, 321.

3. Ren, X.; Pickup, P. G. *J. Phys. Chem.* **1993**, 97, 5356.

4. Qi, Z.; Pickup, P. G. *Chem. Mater.* **1997**, 9, 2934.

Chapter 3 CELL AND REFERENCE ELECTRODE DEVELOPMENT

3.1 INTRODUCTION

In an electrochemical cell, the voltage drop between the working electrode and reference electrode is given by:

$$E_{appl.} = E_{eq.} + \eta + IR_S \qquad (3.1)$$

where $E_{appl.}$ is the external voltage applied by a power supply, $E_{eq.}$ is the equilibrium potential of the working electrode vs the reference electrode, η is the overpotential, and R_S is the solution resistance. IR_S is the ohmic potential drop in the solution, which is an error in the potential control [1]. This error can be minimized by proper cell design, electrode design, and instrumental correction. Traditional three compartment cells reduce the IR_S drop greatly by placing the reference electrode close to the working electrode and passing current through the counter electrode.

A sandwich-type cell was designed in order to minimize IR_S drop and have a cell suitable for studying chemically prepared conducting polymers in various electrolyte solutions, such as in volatile non-aqueous solutions or in dilute high resistance electrolyte solutions.

Commercial reference electrodes, such as SSCE and Ag/AgCl, are too big to be fitted into the sandwich-type cell. In addition, they have the problem of leakage of KCl into

the cell [2]. So a small, stable, non-contaminating reference electrode based on a PPY/PSS-coated fine Pt wire was also designed.

3.2 CELL DESIGN

Figure 3.1 shows a schematic diagram of the sandwich-type cell. The working electrode was a 0.2 cm^2 CFP disk evenly coated with the polymer layer on one side by spreading a slurry with 45% by mass of PTFE binder, using a spatula. The separators consisted of two pieces of Whatman No. 541 filter paper saturated with electrolyte solution (or two Nafion membranes in one experiment) and sandwiching a PPY/PSS-coated fine Pt wire reference electrode. The counter electrode was a 1 cm^2 CFP disk evenly coated with 5 mg of the polymer under study and 45% by mass of PTFE as a binder.

This cell configuration minimizes the distance between the working electrode and the reference electrode and therefore minimizes the uncompensated solution resistance.

3.3 PREPARATION OF THE PT/PPY/PSS REFERENCE ELECTRODES

The PPY/PSS-coated fine Pt wire reference electrodes (Pt/PPY/PSS) were prepared by electrochemically depositing a PPY/PSS film onto a 0.127 mm diameter Pt wire (Aldrich) from an aqueous solution of 0.5 M pyrrole containing 0.1 M NaPSS as the supporting electrolyte. A constant anodic current of 3 mA cm^{-2} was applied for 20 min. The electrode potential during polymerization remained steady at ca. 0.5 V vs SSCE. Multiple electrodes prepared in this way typically exhibited potentials that were reproducible to ±15

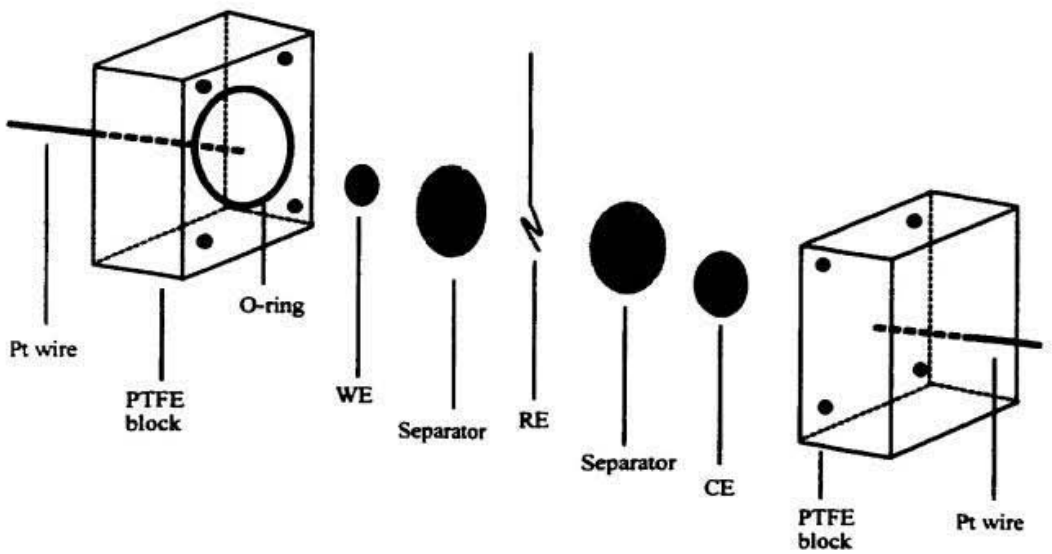

Figure 3.1. Schematic diagram of the sandwich-type cell. WE: working electrode; RE: reference electrode; CE: counter electrode.

mV.

3.4 RESULTS

Excellent cyclic voltammograms of chemically prepared PPY/PSS and PEDOT/PSS in various electrolyte solutions have been obtained with the sandwich-type cell, even in volatile, non-aqueous 0.05 M $LiClO_4$ in CH_3CN (Fig. 3.2). Impedance data were generally satisfactory, although there were sometimes some small variations in the uncompensated resistance with time. Figure 3.3 shows complex plane impedance plots (Nyquist) for chemically prepared PPY/PSS in $LiClO_4$(aq) solutions of various concentrations. These plots approximate ideal behaviour, with almost 45° slopes in the Warburg-like region and very small charge transfer resistances.

For calibration, and to check its stability, the potential of a Pt/PPY/PSS reference electrode was measured against a SSCE in various stirred 0.5 M aqueous electrolyte solutions (Table 1), and in various concentrations of H_2SO_4(aq) (Table 2). In most cases, its potential was stable to within ca. 5 mV for a period of hours after ca. 3 min. Little concentration dependence was observed in H_2SO_4(aq). Calibration of the Pt/PPY/PSS reference electrode was also accomplished in situ by adding ca. 5 mass % of polyvinylferrocene (Polysciences) to the PPY/PSS working electrode (Fig. 3.4). During 10 cycles at 10 mV s^{-1}, the redox peaks of the polyvinylferrocene at ca. 0.12 V drifted very little. This confirms the operational stability of the Pt/PPY/PSS reference electrode.

3.5 CONCLUSIONS

The excellent electrochemical results illustrate that the sandwich-type cell is suitable for electrochemical study of chemically prepared conducting polymers in various electrolyte solutions, even in non-aqueous, volatile, and high resistance electrolyte solutions. The results also show that the PPY/PSS-coated fine Pt wire reference electrode is stable and adequate for the present study where control and knowledge of the potential to better than 10 mV are not important.

Table 1. **Potentials (mV) of a PPY/PSS-coated Pt wire (vs. SSCE) in various 0.5 M aqueous electrolyte solutions.**

Time (min)	H_2SO_4	HCl	$LiClO_4$	$NaClO_4$	LiCl	NaCl	Na_2SO_4	Et_4NCl
5	353	312	262	268	236	217	245	224
35	356	321	250	250	228	215	235	225
95	357	323	249	234	224	212	222	228
155	357	323	250	230	223	210	219	230
215	361	320	251	232	225	215	218	234
935	370	335	228	237	240	224	211	260

Table 2. **Potentials of a PPY/PSS-coated Pt wire (vs. SSCE) after 1 hour in various solutions of H_2SO_4(aq).**

Concentration (M)	0.05	0.10	0.25	0.50	1.0
Potential (mV)	417	415	418	420	420

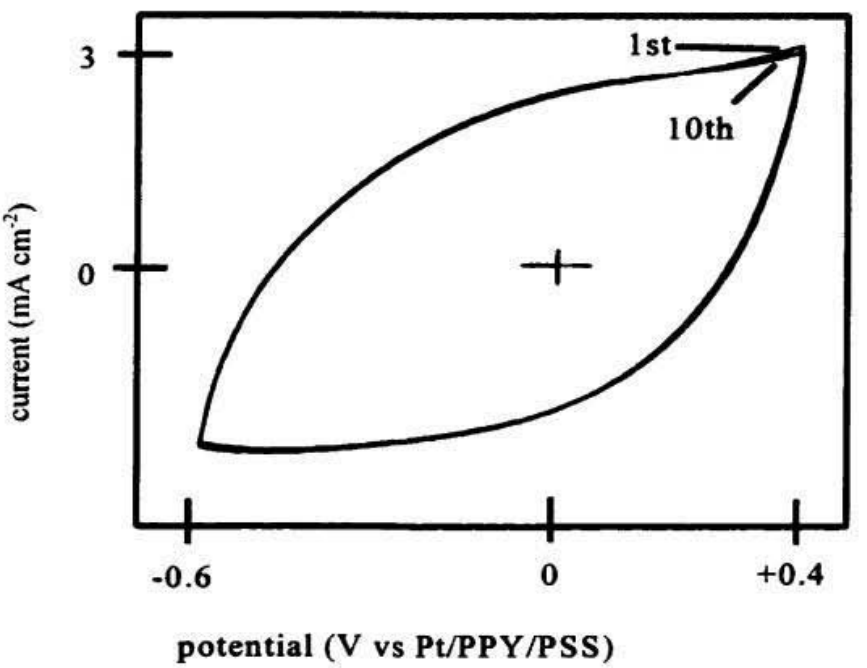

Figure 3.2. Cyclic voltammograms (10 mV s^{-1}) of a chemically prepared PPY/PSS layer (2.5 mg cm^{-2}) in contact with 0.05 M $LiClO_4$+CH_3CN.

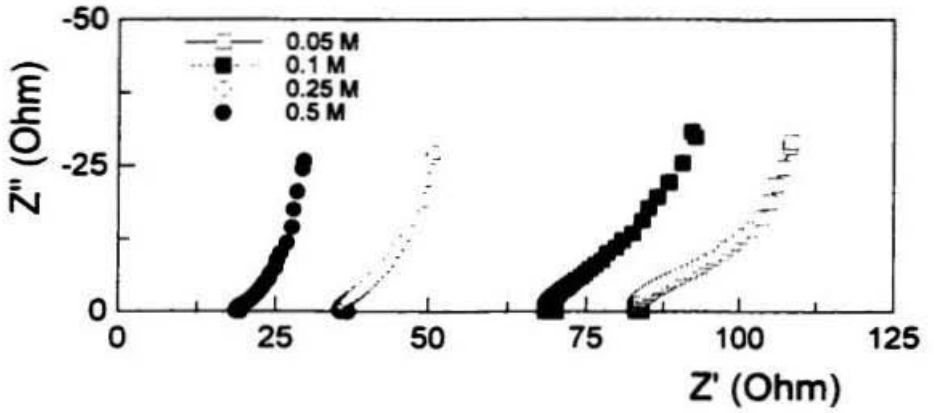

Figure 3.3. Complex plane impedance plots for a chemically prepared PPY/PSS layer (2.5 mg cm^{-2}) in contact with $LiClO_4$(aq) of various concentrations at 0.1 V vs Pt/PPY/PSS.

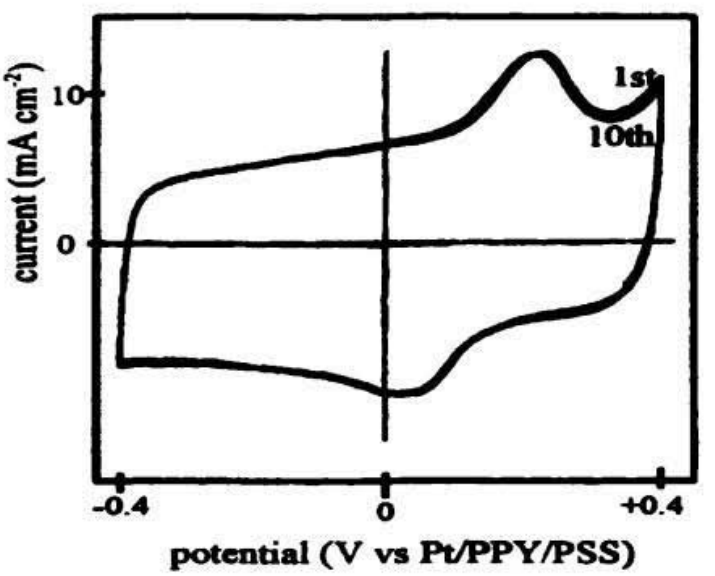

Figure 3.4. Cyclic voltammograms (10 mV s^{-1}) of a chemically prepared PPY/PSS layer (2.5 mg cm^{-2}) containing 5% polyvinylferrocene in contact with 0.5 M LiCl(aq).

References

1. Bard, A.; Faulkner, L.R. *Electrochemical Methods*; John Wiley & Sons: New York, 1980; p22.

2. Skoog, D. A.; Leary, J. J. *Principles of Instrumental Analysis*; Saunders College Publishing: New York, 1992; p489.

Chapter 4 ION TRANSPORT IN CHEMICALLY PREPARED POLYPYRROLE/POLY(STYRENE-4-SULFONATE) COMPOSITES

4.1 INTRODUCTION

Polypyrrole/poly(styrene-4-sulfonate) (PPY/PSS) composites have attracted much interest in recent years [1-4]. With the advantages of high electronic and ionic conductivity, and particularly high proton conductivity, they have great potential in applications such as batteries, supercapacitors and fuel cells [4-6].

PPY/PSS can be easily prepared both electrochemically [7] and with chemical oxidants [8] as illustrated in Equation 4.1, although the properties of the resulting polymer, such as ion transport and morphology, may be significantly different. Qi and coworkers [4] have found that the ionic conductivities of packed layers of chemically prepared

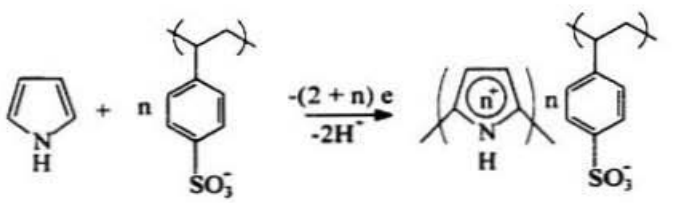

(4.1)

PPY/PSS (c-PPY/PSS) are much higher than those of electrochemically prepared PPY/PSS (e-PPY/PSS) films. The c-PPY/PSS powder exhibited proton conductivity as high as 0.03 S cm^{-1} when pressed as 50 μm layer on a Nafion proton-conducting membrane, which is

100 times higher than the proton conductivity of e-PPY/PSS immersed in 1M H_2SO_4(aq).

Because the PSS counter-ions are trapped in the PPY polymer matrix during synthesis, cations must move into, or out of, the PPY/PSS composite during discharge and recharge, as shown in Equation 4.2. PPY/PSS is therefore permselective to cations. Experimental results have shown that its ion transport is dominated by cation transport [2,9-10].

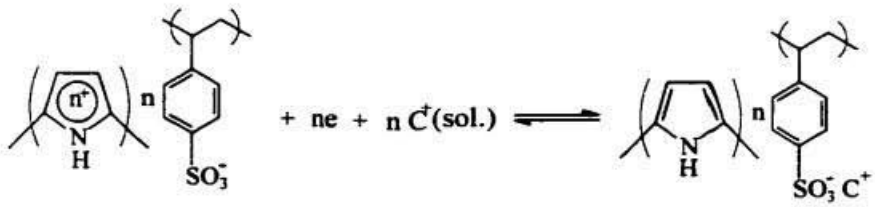

(4.2)

The electrochemistry of PPY/PSS and many of its applications involve both electron and ion transport, as illustrated in Equation 4.2, so fully understanding its ion transport properties is crucial to understanding its electrochemistry and optimizing its applications. Furthermore, the study of ionic conductivity can provide valuable insight into the structure of PPY/PSS film [11].

Previously, the study of ion transport in PPY/PSS has been focused on electrochemically prepared samples [11]. This chapter will report ion transport in chemically prepared PPY/PSS in various electrolyte solutions. Ionic conductivities have been determined by impedance spectroscopy. The incorporated ions were analysed by elemental analysis and X-Ray emission analysis (EDX). The morphology of PPY/PSS was observed with scanning electron microscopy (SEM). The combination of these data

provides a clear picture of ion transport in c-PPY/PSS and explains why it has such high ionic conductivity relative to its electrochemically prepared counterpart and why it has extraordinarily high proton conductivity.

4.2 RESULTS AND DISCUSSION

4.2.1 Preparation of PPY/PSS Composites

The PPY/PSS composites were prepared as previously reported [3], by chemical oxidation of 50 mL of 0.13 M aqueous pyrrole containing 0.04 M sodium poly(styrene-4-sulfonate) with 50 mL of 0.6 M $Fe(NO_3)_3$ in 0.06 M HNO_3(aq). After 80 minutes the black precipitate was collected by filtration, washed copiously with water, and dried at room temperature under vacuum.

4.2.2 Composition of PPY/PSS Composites

The composition of one sample of the PPY/PSS composite was analysed by Canadian Microanalytical Services and the results are shown in Table 4.1.

Table 4.1. Elemental analysis of a PPY/PSS composite.

Element	C	H	N	O	S	Fe	Total
Determined	52.28%	4.09%	11.91%	18.82%	5.13%	1.2%[a]	93.43%
Calculated	55%	4%	12%	20%	6%	2%	99%

a: From EDX

The S:N ratio, which should represent the relative composition of PSS:PY units and therefore a indirect measure of the degree of oxidation, is 0.19, which is essentially the same as that obtained in a previous synthesis [3] under similar conditions. However, the total analysis accounted for only 92.23% of the mass. X-Ray emission analysis (Fig. 4.1) indicated the additional presence of iron. Based on the Fe/S ratio from EDX analysis and the % S from elemental analysis, the sample can be estimated to contain 1.2% Fe by mass. This Fe is presumably in the form of Fe^{3+} counter-ions (presumably as $Fe(H_2O)_6^{3+}$) associated with PSS in the composite. A charge balance, and global fitting of the analytical results indicated that there is also NO_3^- in the composite. A composition of $PPY(PSS)_{0.25}Fe_{0.05}(NO_3)_{0.15}\cdot 0.4H_2O$, corresponding to a PPY degree of oxidation of 0.25, fits the analytical data reasonably well (Table 4.1). The use of only one or two significant figures reflects the uncertainty caused by the low total analysis. The Fe analysis is assumed to be the least accurate. The Fe^{3+} and NO_3^- cannot be washed from the PPY/PSS composite, presumably because the Fe^{3+} is strongly associated with the PSS. Alternatively, the Fe^{3+} may be in PSS-rich regions of the composite while the NO_3^- is in PPY-rich regions [12].

4.2.3 Electronic Conductivities of the Dry PPY/PSS Powders

The electronic conductivities of the dry PPY/PSS powders were measured with a modified four-point probe in which the polymer is pressed into a pellet. The conductivities of the dry polymer decreased greatly over a period of a year, from the initial value of 0.21 S cm^{-1} to 0.018 S cm^{-1}. The degradation of conductivity with time is the common drawback

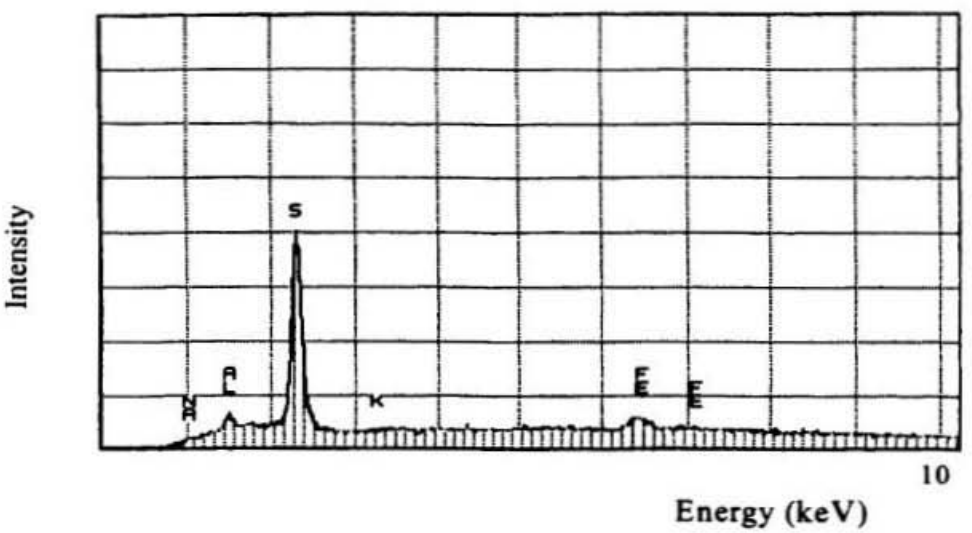

Figure 4.1. EDX spectrum of a c-PPY/PSS sample.

of conducting polymers, and is presumably due to nucleophilic attack by atmospheric water [13]. A second sample of PPY/PSS had an initial conductivity of 0.19 S cm^{-1}.

4.2.4 Conductivities of the Electrolyte Solutions

The conductivities (σ_{sol}) of the aqueous electrolyte solutions were measured by impedance spectroscopy in a standard conductivity cell. The following equation was used:

$$\sigma_{sol} = \sigma_{KCl} \times R_{KCl} / R_{sol} \qquad (4.3)$$

σ_{KCl} (= 112 mS cm^{-1} [14]) is the conductivity of 1 M KCl, R_{KCl} is the ionic resistance with 1M KCl in the cell, and R_{sol} is the resistance of the solution. The results are listed in Table 4.2. They are consistent with literature values [14].

Table 4.2. Ionic conductivities (mS cm^{-1}) of the aqueous electrolyte solutions employed.

Conc.(M)	0.05	0.075	0.10	0.125	0.25	0.50	0.75	1.0
H_2SO_4	28.3	40.3	53.7	63.4	112	204	273	350
HCl	22.7	31.7	44.8	47.3	85.0	129	179	257
Na_2SO_4	9.1		18		29	51		
$LiClO_4$	4.1		8.4		18	34		
$NaClO_4$	5.8		12		21	41		
LiCl	4.1		9.0		18	34		
NaCl	5.8		12		21	41		
Et_4NCl	3.6		7.3		12	26		

4.2.5 Morphologies of PPY/PSS Samples

The morphologies of PPY/PSS films and powders were studied by scanning electron microscopy. The e-PPY/PSS film was obtained by depositing PPY/PSS on a 0.071 cm^2 glassy carbon electrode from a 0.5 M aqueous pyrrole solution containing 0.1 M NaPSS. A constant anodic current of 60 μA was applied for 20 minutes. The potential during electrolysis remained steady at ca. 0.47 V (vs SSCE). The SEM micrographs (Fig. 4.2) clearly show that the c-PPY/PSS powder is more porous than the e-PPY/PSS film.

4.2.6 Cyclic Voltammetry

The electrochemical properties of the PPY/PSS composites were investigated in various electrolyte solutions with the sandwich-type cell described in Ch.3. Figures 4.3, 4.4, and 4.5 show cyclic voltammograms of PPY/PSS-coated carbon fibre paper electrodes in aqueous 0.1 M H_2SO_4 and 0.5 M Et_4NCl solutions, and a non-aqueous 0.5 M $LiClO_4$ in CH_3CN solution, respectively. The potential scan range was restricted to ±0.5 V vs the Pt/ PPY/PSS reference electrode to avoid degradation of the polymer. The cyclic voltammograms in different electrolyte solutions (Fig. 4.3, 4.4, and 4.5) are all similar, and similar voltammetric properties were also observed in aqueous solutions of HCl, $LiClO_4$, $NaClO_4$, NaCl, LiCl, and Na_2SO_4. The cyclic voltammograms are all unremarkable with large capacitance-like currents, which are characteristic of conducting polymers. The current peaks normally seen in cyclic voltammograms of polypyrrole are beyond the lower potential limit used in this work [4].

(a)

(b)

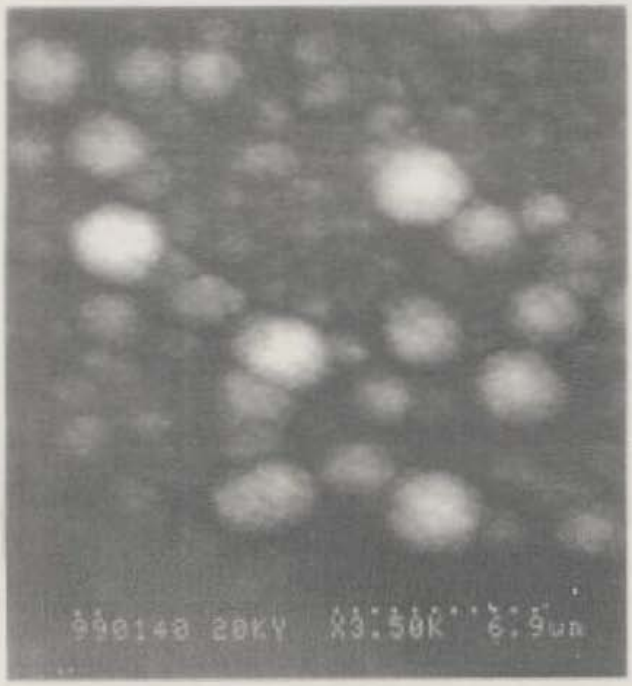

Figure 4.2. SEM micrographs of (a) c-PPY/PSS and (b) e-PPY/PSS.

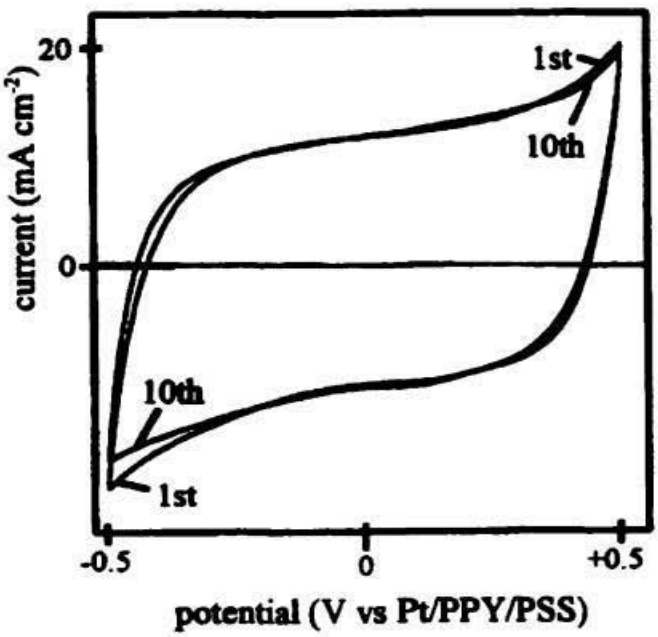

Figure 4.3. Cyclic voltammograms (20 mV s^{-1}) of a c-PPY/PSS layer (2.5 mg cm^{-2}) in contact with 0.1 M H_2SO_4(aq).

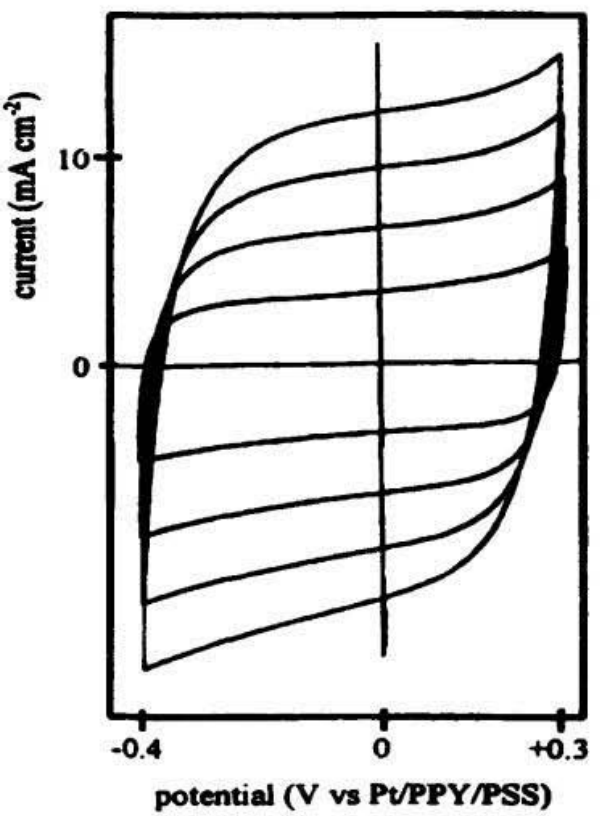

Figure 4.4. Cyclic voltammograms (10, 20, 30, and 40 mV s^{-1}) of a c-PPY/PSS layer (2.5 mg cm^{-2}) in contact with 0.5 M Et_4NCl(aq).

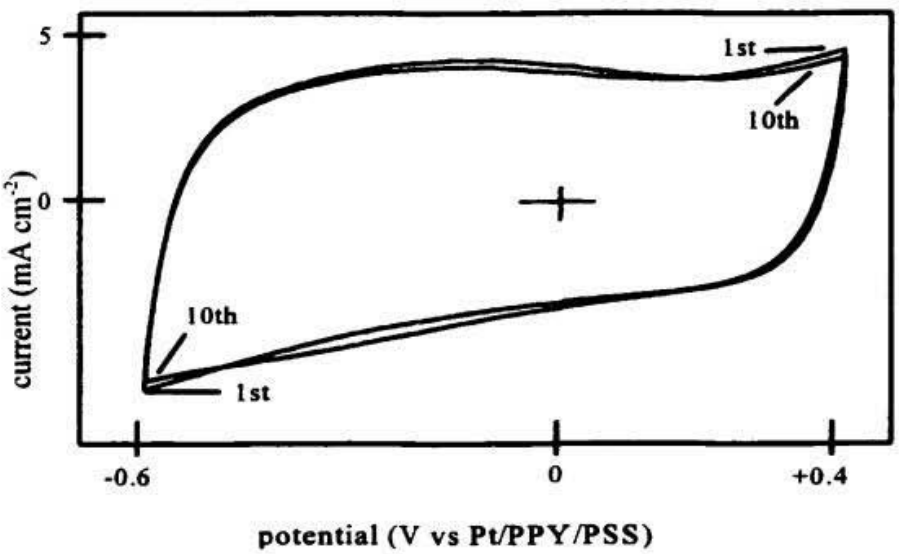

Figure 4.5. Cyclic voltammograms (10 mV s^{-1}) of a c-PPY/PSS layer (2.5mg cm^{-2}) in contact with 0.5 M $LiClO_4$+CH_3CN.

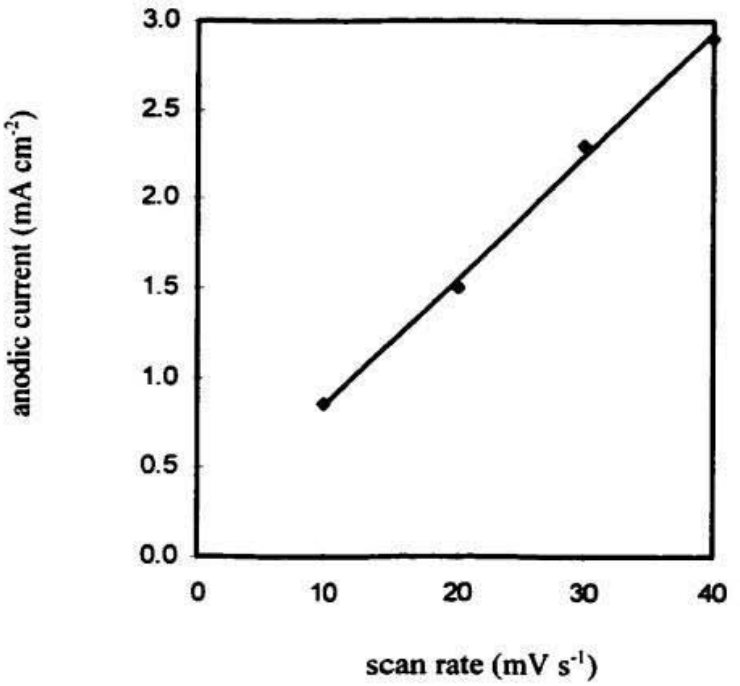

Figure 4.6. Anodic currents (at 0 V vs Pt/PPY/PSS) of a c-PPY/PSS layer (2.5 mg cm^{-2}) in 0.5 M $Et_4NCl(aq)$ at scan rates of 10, 20, 30, and 40 mV s^{-1}.

The cyclic voltammograms of PPY/PSS in the above electrolytes show only very small change through multiple cycles over the ±0.5 V potential range (e.g. Fig. 4.3 and 4.5). This demonstrates the good stability of the PPY/PSS composite. Voltammetric currents increase almost linearly with increasing scan speed, even with the bulky Et_4N^+ counter-ion (Fig. 4.6). This indicates that both ion and electron transport in PPY/PSS are fast. Currents also increase with increasing loading of PPY/PSS on the electrode (i.e., increasing layer thickness). This is illustrated in Table 4.3, which lists charges and specific Faradaic pseudocapacitances from voltammograms at 10 mV s^{-1} in 0.5 M H_2SO_4(aq) as a function of PPY/PSS loading. The capacitances were calculated from the averages of the anodic and cathodic currents at 0 V in the 10 mV s^{-1} voltammograms by using the following equation:

specific capacitance = average current/(scan rate x mass of polymer) (4.4)

Table 4.3. Voltammetric charges and specific capacitances in 0.5 M H_2SO_4(aq) for various loadings of PPY/PSS on a 0.2 cm^2 electrode.

PPY/PSS loading (mg)	0.5	1.0	1.5	2.0
Voltammetric charge[a] (mC)	55	163	224	268
Specific capacitance (F g^{-1})	170	250	253	230

a. for an anodic scan from -0.4 to +0.3 V at 10 mV s^{-1}

At the lowest loading (2.5 mg cm^{-2}) the voltammetric charge and capacitance are both low relative to the higher loadings (Table 4.3). This is presumably due to the loss of some of the polymer into cavities in the hydrophobic CFP support, where the polymer is

isolated from the solution and therefore not electrochemically active. At intermediate loadings (5 to 7.5 mg cm^{-2}) the voltammetric charge scales linearly with loading, and the specific capacitance is constant. However, at higher loading (10 mg cm^{-2}) the voltammetric charge begins to level off, and the specific capacitance falls, as the time required to charge and discharge the layer becomes longer than the cycle time. Voltammetric charges and specific Faradaic pseudocapacitances showed little dependence on the electrolyte employed (Table 4.4).

Table 4.4. Specific Faradaic pseudocapacitances (F g^{-1}) at +0.1 V (vs Pt/PPY/PSS), from 10 mV s^{-1} cyclic voltammetry and impedance spectroscopy on 2.5 mg cm^{-2} PPY/PSS layers in various 0.5 M aqueous electrolyte solutions.

Electrolyte	H_2SO_4	HCl	$LiClO_4$	LiCl	$NaClO_4$	NaCl	Na_2SO_4	Et_4NCl
Voltammetry	170	150	165	140	155	150	150	150
Impedance	135	115	145	90	125	100	110	110

The 7.5 mg cm^{-2} loading corresponds to a polymer layer thickness of ca. 0.16 mm, and it is surprising that such a thick layer is fully electrochemically active (Fig.4.7). Since electroactivity of the polymer layer requires facile ion transport as well as good electronic conductivity, this result illustrates the excellent ion transport characteristics of the PPY/PSS composite layer.

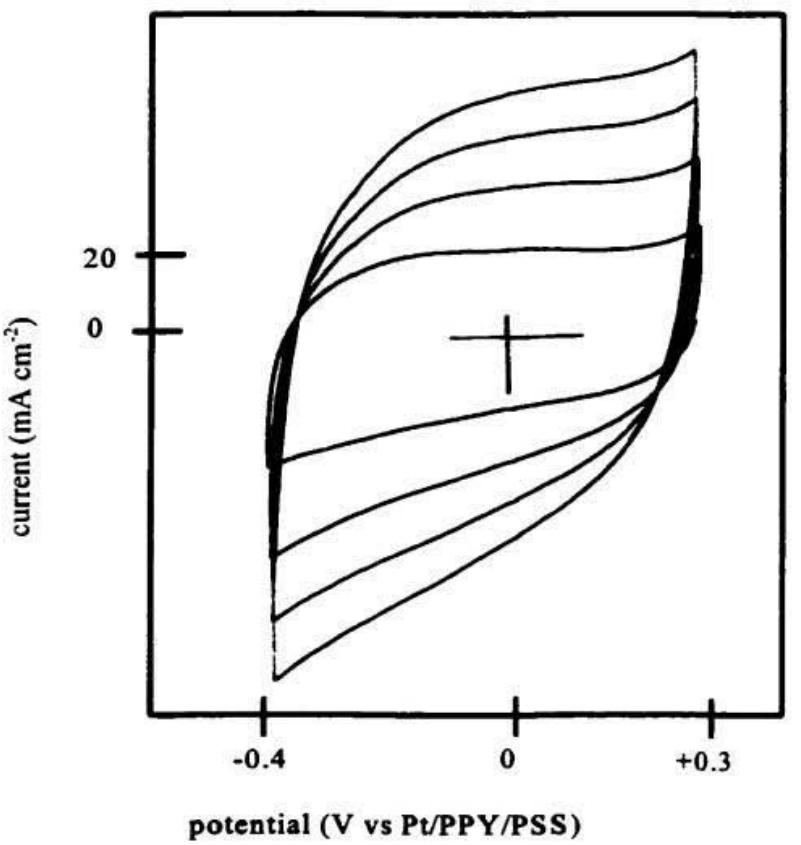

Figure 4.7. Cyclic voltammograms (10, 20, 30, and 40 mV s^{-1}) of a c-PPY/PSS layer (7.5 mg cm^{-2}) in contact with 0.5 M H_2SO_4(aq).

4.2.7 Impedance Spectroscopy

The ionic conductivities of PPY/PSS layers in various aqueous electrolyte solutions (H_2SO_4, HCl, $LiClO_4$, LiCl, $NaClO_4$, NaCl, Na_2SO_4, and Et_4NCl) and a non-aqueous solution ($LiClO_4$ in CH_3CN) have been determined by impedance spectroscopy as a function of both concentration and applied potential. This type of broad study provides insight into both the nature of the ion transport processes in a polymer layer and the structure of the layer [11].

Ionic resistances were obtained from impedance data by using Equation 2.1, and then converted to ionic conductivities according to Equation 2.2. The thickness of a 2.5 mg cm^{-2} dry PPY/PSS layer was measured as 55 μm with a micrometer. The actual thickness of the polymer layer in solution may be somewhat higher due to the swelling effect of the solvent. Resistances increased with increasing loading to 7.5 mg cm^{-2} (satisfactory impedance plots were not obtained at 10 mg cm^{-2}), with conductivities of 17, 28, and 18 mS cm^{-1}, respectively, being obtained for 2.5, 5.0, 7.5 mg cm^{-2} loadings in 0.5 M H_2SO_4(aq). All subsequent experiments were conducted with a polymer loading of 2.5 mg cm^{-2}.

An illustrative set of impedance data at different electrolyte concentrations is shown in Figure 4.8. The general shape of these complex plane impedance plots approximates the behaviour of a finite transmission line, as predicted theoretically [15]. The length of the Warburg-like region (almost 45° slope) increases with decreasing concentration of the electrolyte. This indicates that the ionic resistance of the polymer layer increases with decreasing concentration of the electrolyte. Similar behaviour was also observed in other

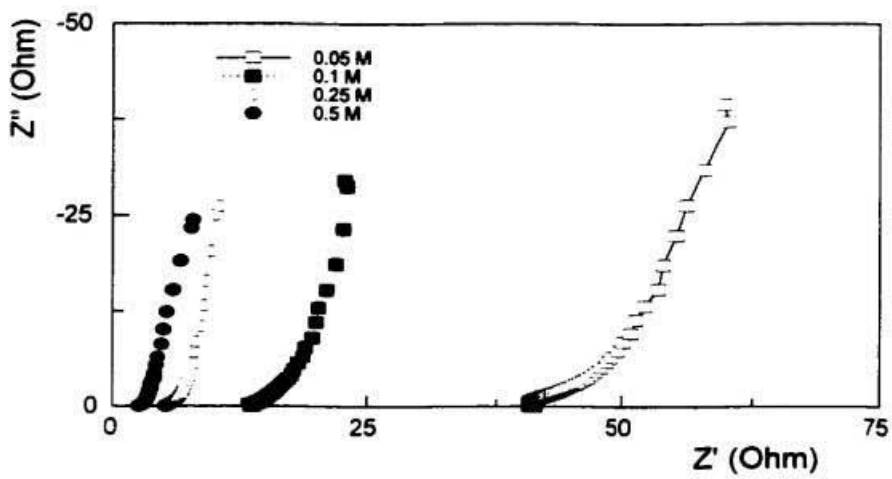

Figure 4.8. Complex plane impedance plots at 0.1 V vs Pt/PPY/PSS for a c-PPY/PSS layer (2.5 mg cm^{-2}) in contact with H_2SO_4(aq) of various concentrations.

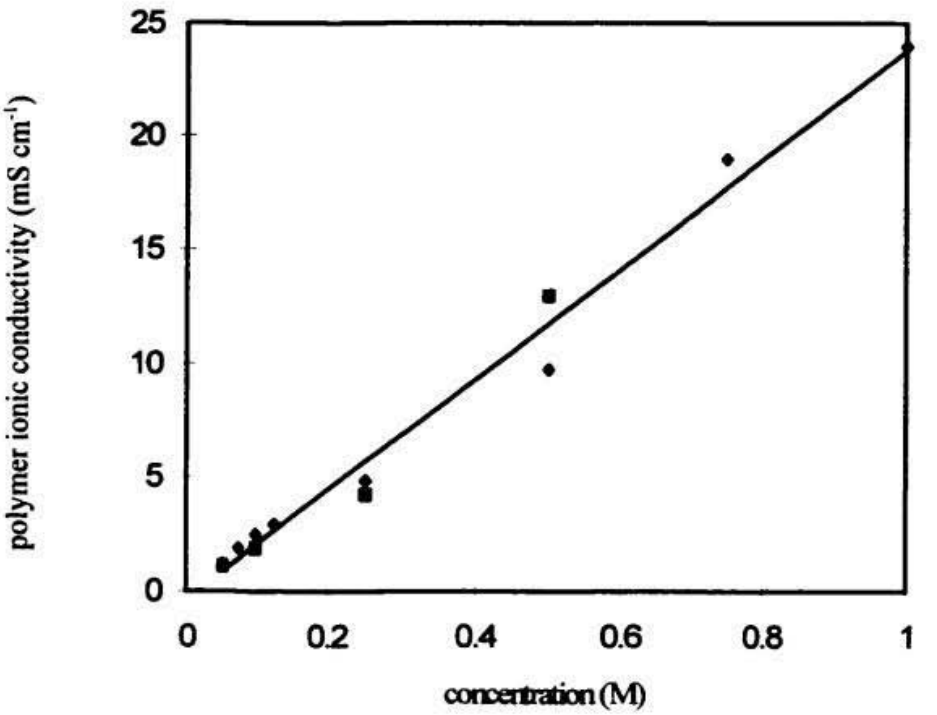

Figure 4.9. Ionic conductivity of c-PPY/PSS at 0.1 V vs Pt/PPY/PSS as a function of electrolyte concentration in H_2SO_4(aq). Data for two different electrodes are shown (■ and ♦), together with a linear least squares fit of all of the data. R^2 is ca. 0.99.

electrolyte solutions (Table 4.5).

Figure 4.9 shows the ionic conductivity of the polymer as a function of electrolyte concentration in H_2SO_4(aq). Data for two different electrodes are shown, together with a linear least squares fit of all of the data. The strong dependance of the polymer layer's ionic conductivity on the electrolyte concentration shows that it is dominated by electrolyte in pores [11]. The y-intercept of the plot is close to zero (slightly negative) indicating that the intrinsic ionic conductivity of the polymer (i.e., in the absence of electrolyte in pores) is too small to assess accurately from these data (i.e., < 1 mS cm^{-1}).

The ionic conductivity of the polymer shows no clear dependence on the nature of the electrolyte but correlates well with its conductivity. This is illustrated in Figure 4.10 where the ionic conductivity of the polymer is plotted against the conductivity of the electrolyte for various electrolytes and concentrations. Again, these data show that the polymer layer's ionic conductivity is dominated by electrolyte in pores. The intercept of the linear least squares fit through all the data suggests that the intrinsic ionic conductivity of the polymer phase is ca. 0.2 mS cm^{-1}.

The slope of the linear regression in Fig. 4.10 shows that the ionic conductivity of the polymer layer is on average 5% of the solution conductivity. In contrast, electrochemically prepared films of PPY/PSS exhibit only 0.5% of the bathing solution's conductivity [11]. The clear conclusion from this comparison is that chemically prepared PPY/PSS is much more porous than the electrochemically prepared counterpart, and this is supported by the scanning electron microscopy images (Fig. 4.2).

Table 4.5. Ionic conductivities (mS cm^{-1}) of PPY/PSS layers in various electrolyte solutions at 0.1 V vs Pt/PPY/PSS.

Conc. (M)	0.05	0.075	0.10	0.125	0.25	0.50	0.75	1.0
H_2SO_4(aq)	1.2	1.9	2.5	2.9	4.8	9.7	19	24
HCl(aq)	0.9	1.4	2.4	2.8	4.2	6.9	9.7	11
$LiClO_4$(aq)	0.56		0.79		1.1	1.5		
$LiClO_4$+CH_3CN	0.71		0.95		1.3	1.9		
LiCl(aq)	0.23		0.43		1.1	1.5		
$NaClO_4$(aq)	0.44		0.66		1.5	2.6		
NaCl(aq)	0.31		0.52		1.1	2.0		
Na_2SO_4(aq)	0.49		0.84		2.1	4.2		
Et_4NCl(aq)	0.34		0.50		0.84	1.3		

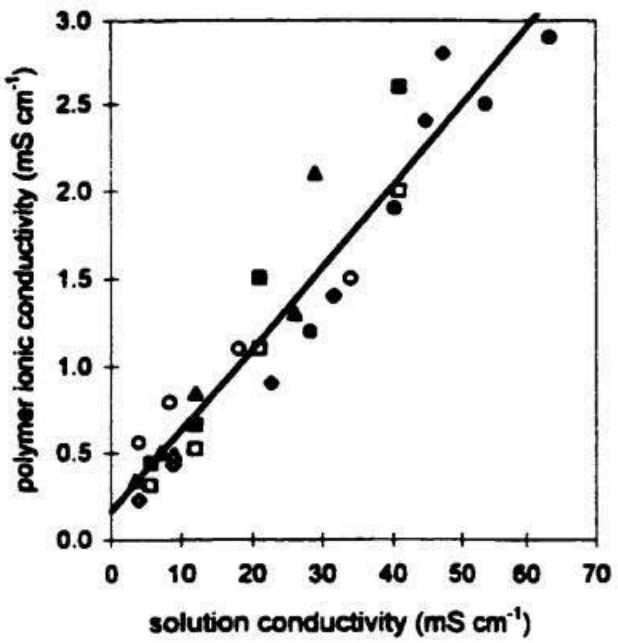

Figure 4.10. Ionic conductivity of c-PPY/PSS at 0.1 V vs Pt/PPY/PSS in aqueous solutions of H_2SO_4 (•), HCl (♦), $LiClO_4$ (◦), LiCl (◇), $NaClO_4$ (■), NaCl (□), Na_2SO_4 (△), and Et_4NCl (▲), as a function of electrolyte conductivity. R^2 is ca. 0.91.

The ionic conductivities of the polymer in non-aqueous $LiClO_4$+CH_3CN solutions are significantly higher than in aqueous $LiClO_4$ solutions of same concentration (Figure 4.11). This is presumably due to the strong solvation of Li^+ in water.

The ionic conductivity of c-PPY/PSS was found to be virtually independent of potential in high concentration solutions studied (e.g. Fig. 4.12), indicating again that it is dominated by electrolyte solution in pores [11]. However in low concentration solutions, there was a slight dependence. The ionic conductivity of the layer increases as the polymer is reduced, because more mobile counter-ions are inserted. Thus, at low electrolyte concentrations, the ionic conductivity of the polymer phase begins to become significant.

Low frequency capacitances from all sets of impedance data were consistent with those from cyclic voltammetry (Table 4.4), although 20% lower as is typically observed for conducting polymers [16].

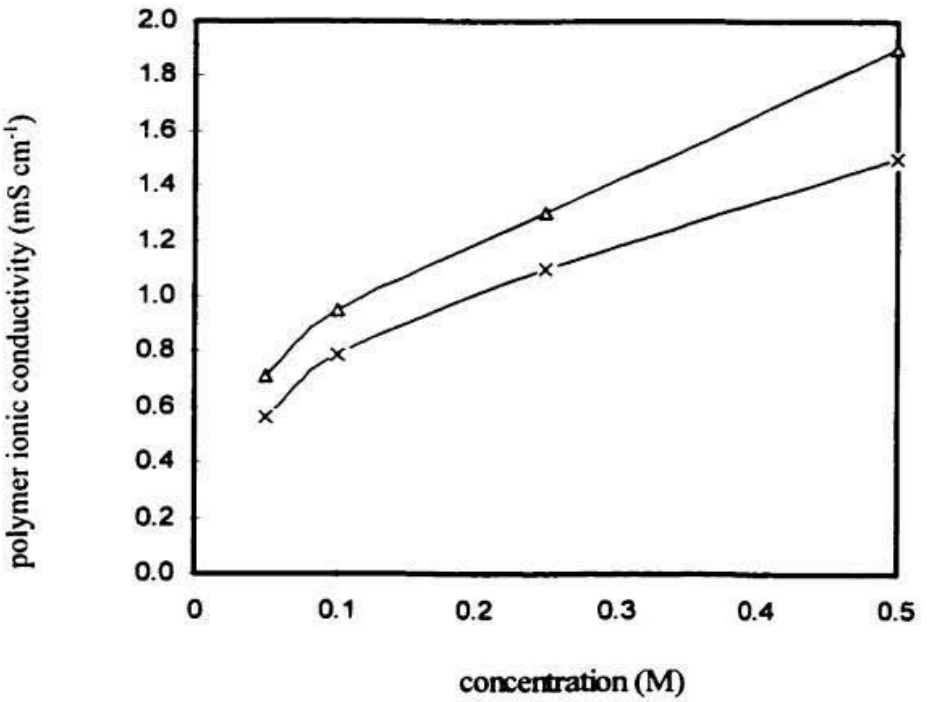

Figure 4.11. Ionic conductivities of a c-PPY/PSS layer (2.5 mg cm^{-2}) in (△) $LiClO_4$+CH_3CN and (x) $LiClO_4$(aq) of various concentrations at 0.1 V vs Pt/PPY/PSS.

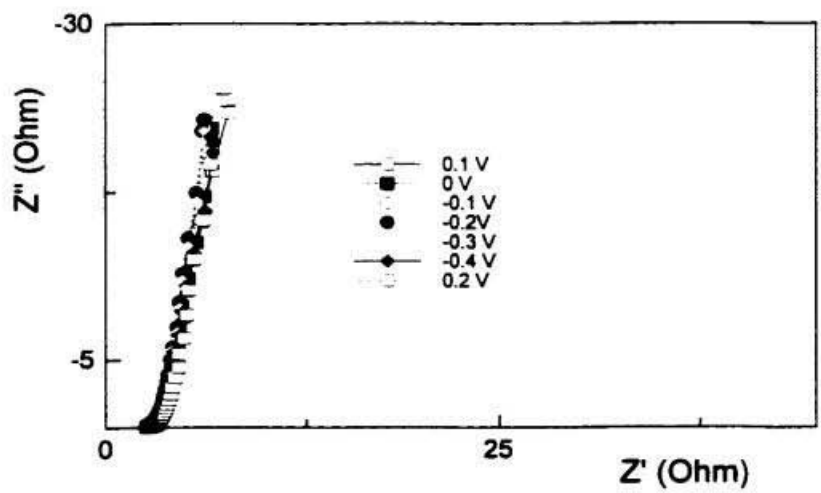

Figure 4.12. Complex plane impedance plots for a c-PPY/PSS layer (2.5 mg cm^{-2}) at various applied potentials vs Pt/PPY/PSS in contact with 0.5 M H_2SO_4(aq).

4.2.8 Use of Nafion Membranes as the Electrolyte

The conclusion that the high ionic conductivity of chemically prepared PPY/PSS is due to electrolyte in pores leaves unanswered the question of why high ionic conductivities were observed in gas diffusion electrodes without access of liquid electrolyte to the polymer layer [4]. Presumably, the pores in the polymer layer must fill with liquid electrolyte in some way. To investigate this further, and to rule out the remote possibility that electrolyte crossed the membrane in the previous experiments, Nafion 117 membranes were used as the electrolyte in the sandwich-type cell (Fig.3.1) instead of the electrolyte-soaked filter papers. The membranes were equilibrated in water at 22 °C before use to ensure that they were well hydrated, but no electrolyte solution was used. Typical impedance data are shown in Fig. 4.13. From these results the ionic conductivity of the c-PPY/PSS layer can be estimated to be 3 mS cm^{-1}, with a slight dependence on potential. This is similar to values reported by Qi and coworkers [4] for a c-PPY/PSS layer that was separated from a 1 M H_2SO_4(aq) solution by a Nafion membrane, although significantly higher values (ca. 25 mS cm^{-1}) were obtained when 0.1 M H_2SO_4(aq) was employed [4].

Our results with liquid electrolytes indicate that the high ionic conductivities of c-PPY/PSS layers in contact with Nafion membranes must be due to liquid electrolyte in the c-PPY/PSS layer. The inherent ionic conductivity of the c-PPY/PSS composite (i.e., of the polymer phase) is clearly insufficient to explain the observed values of 3 mS cm^{-1} or more. How then does this liquid electrolyte originate?

The PTFE suspension used as a binder was quickly ruled out, and leakage of

electrolyte from elsewhere is not possible in the cell used in this work (with Nafion separators). The liquid electrolyte in the c-PPY/PSS layer must therefore originate from the Fe^{3+} and NO_3^- counter-ions that could not be removed by washing. Microprobe analysis showed that when a c-PPY/PSS layer is placed in contact with a Nafion membrane, much of the Fe^{3+} is replaced by H^+ from the Nafion (Figure 4.14). Since the H^+ is not required to compensate the charge on the PSS, it will be present in the PPY/PSS layer as HNO_3(aq), and will therefore provide a high ionic conductivity. From the analytical results (the moles of H^+ in the polymer layer/the volume of the polymer layer), it can be estimated that the equivalent of ca. 0.5 M HNO_3 will be formed in the full volume of the PPY/PSS layer. This is clearly sufficient to produce the observed conductivities. The HNO_3 concentration will be even higher if HNO_3(aq) is formed only in pores.

4.2.9 Morphology of Chemically Prepared PPY/PSS Layers

Based on the ionic conductivity data, the morphologies of chemically prepared PPY/PSS layers can be represented by a model proposed by Ren and Pickup [11] for electrochemically prepared PPY films (Fig. 4.15). That is, the polymer layer consists of permselective polymer aggregates (polymer phase) which enclose pores containing electrolyte solution. According to this model, ion transport in a polymer layer involves ions both in the polymer phase and through electrolyte in the pores. In high concentration electrolyte solutions, ion transport is dominated by electrolyte in the pores, while in low concentration electrolyte solutions, ion transport in the polymer phase becomes significant.

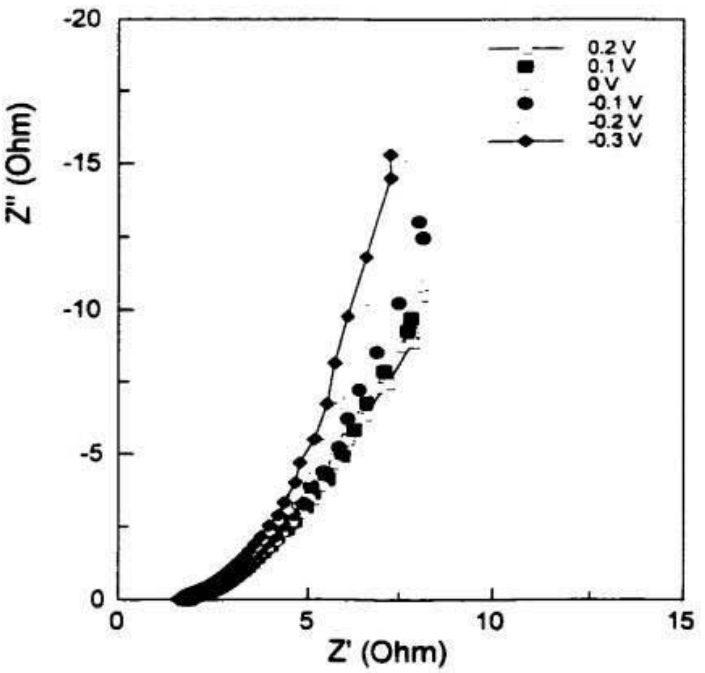

Figure 4.13. **Complex plane impedance plots for a c-PPY/PSS layer (2.5 mg cm^{-2}) in pressure contact with a hydrated Nafion membrane (potentials vs Pt/PPY/PSS).**

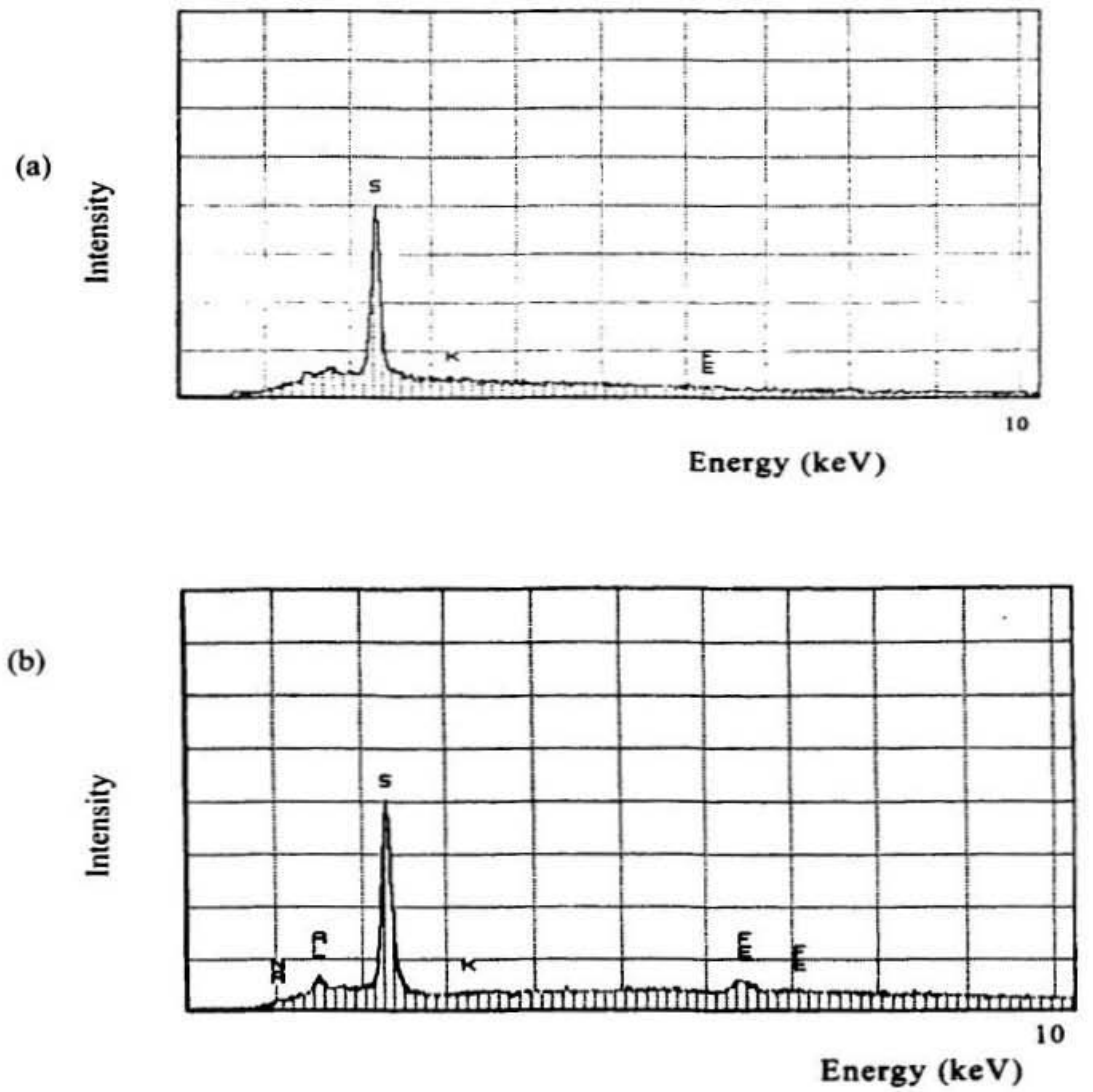

Figure 4.14. EDX spectra of c-PPY/PSS: a. after 12 hours in contact with a Nafion membrane, b. without exposure to a Nafion membrane.

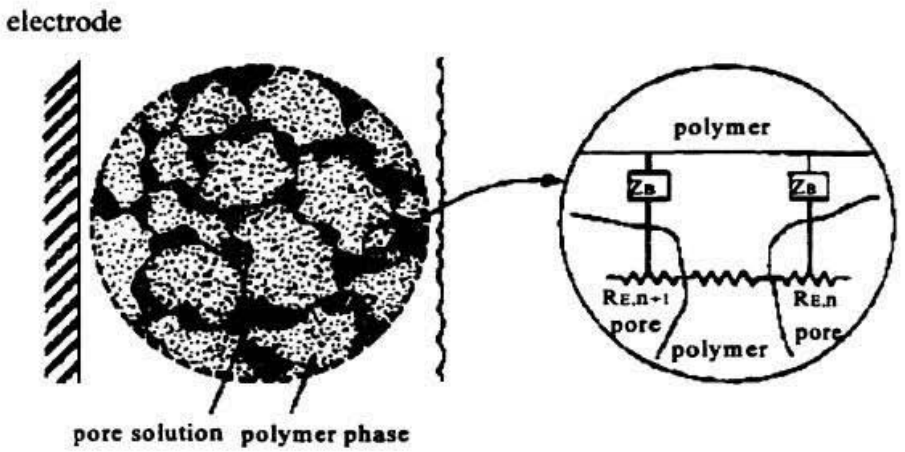

Figure 4.15. A morphological model for PPY/PSS layers and films, and the corresponding equivalent circuit [11].

4.3 CONCLUSIONS

The facile electrochemistry of chemically prepared PPY/PSS composites has been shown to be due to the high ionic conductivity of electrolyte within their very porous structures. The extraordinarily high proton conductivity of chemically prepared PPY/PSS is due to the extraordinarily high ionic conductivity of H^+. Layers of the chemically prepared composites are approximately ten times more porous than electrochemically prepared films, and therefore have ionic conductivities that are higher by a similar factor. The morphologies of chemically prepared PPY/PSS layers are similar to those of electrochemically prepared PPY/PSS films but more porous. The high ionic conductivities previously obtained for PPY/PSS layers bonded to Nafion membranes have been shown to be likely due to HNO_3 generated in pores by ion exchange of residual Fe^{3+} with H^+ in the Nafion.

References

1. Iyoda, T.; Ohtani, A; Shimidzu, T.; Honda, K. *Chem. Lett.* **1986**, 687.

2. Ren, X.; Pickup, P. G. *J. Phys. Chem.* **1993**, 97, 5356.

3. Qi, Z.; Pickup, P. G. *Chem. Mater.* **1997**, 9, 2934.

4. Qi, Z.; Lefebvre, M. C.; Pickup, P. G. *J. Electroanal. Chem.* **1998**, 459, 9.

5. Tsutsumi, H.; Yamashita, S.; Oishi, T. *J. Appl. Electrochem.* **1997**, 27, 477.

6. Qi, Z.; Pickup, P. G. *Chem. Commun.* **1998**, 15.

7. Otero, T. F.; Sansinena, J. M. *J. Electroanal. Chem.* **1996**, 412, 109.

8. Arribas, C.; Rueda, D. *Synth. Met.* **1996**, 79, 23.

9. Baker, C. K.; Qiu Y. J.; Reynolds, J. R. *J. Phys. Chem.* **1991**, 95, 4446.

10. Naoi, K.; Lien, M.; Smyrl, W. H. *J. Electrochem. Soc.* **1991**, 138, 440.

11. Ren, X.; Pickup, P. G. *J. Electroanal. Chem.* **1995**, 396, 359.

12. Ren, X.; Pickup, P. G. *Electrochim. Acta* **1996**, 41, 1877.

13. Pud, A. A. *Synth. Met.* **1994**, 66, 1.

14. Skoog, D. A. *Principles of Instrumental Analysis*, 3rd ed.; CBS College Publishing: New York, 1985; p708.

15. Albory, W. J.; Mount, A. R. In *Electroactive Polymer Electrochemistry, Part 1: Fundamentals*; Lyon, M. E. G., Ed.; Plenum Press: New York, 1994; pp. 443-483.

16. Ren, X.; Pickup, P. G. *J. Electroanal. Chem.* **1994**, 372, 289.

Chapter 5 ION TRANSPORT IN POLY(3,4-ETHYLENEDIOXY-THIOPHENE)/POLY(STYRENE-4-SULFONATE) COMPOSITES

5.1 INTRODUCTION

Poly(3,4-ethylenedioxythiophene) (PEDOT) has been found to have high conductivity, and appears to be the most stable conducting polymer currently available [1]. It has therefore attracted much interest in recent years [2-3]. PEDOT is currently being marketed by Bayer, and has been studied for many applications, such as electrochromic devices [4], biosensors [5], supercapacitors [2], and batteries [6].

When PEDOT is synthesized in the presence of poly(styrene-4-sulfonate) (PSS), PSS is incorporated into the polymer to compensate the positively charged PEDOT (Equation 5.1), and becomes trapped in the polymer matrix.

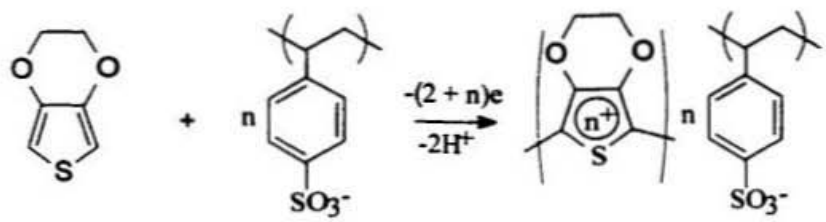

(5.1)

The discharge and recharge of the resulting polymer is expected to involve cations moving into, or out of, the polymer as shown in Equation 5.2. PEDOT/PSS is therefore

assumed to be permselective to cations when partially or fully discharged. The validity of these concepts will be explored in this chapter. Knowledge of ion transport in PEDOT/PSS is crucial to understanding its electrochemistry and optimizing many of its applications. Furthermore it can shed light on the morphology of PEDOT/PSS composites.

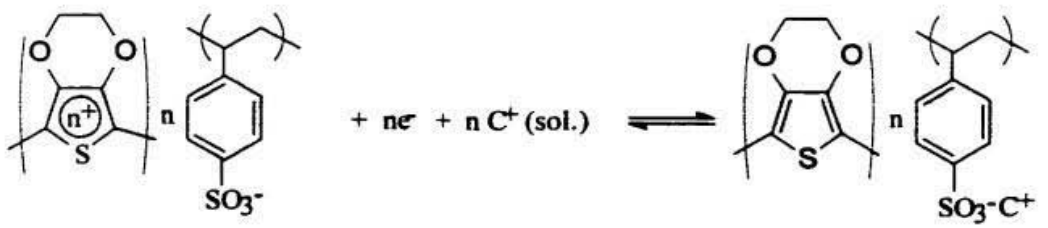

(5.2)

PEDOT/PSS composites exhibiting high electronic conductivity have been synthesized both electrochemically and with chemical oxidants [3,6]. However little data are available about their ion transport properties. This chapter reports ion transport in both chemically prepared PEDOT/PSS (c-PEDOT/PSS) and electrochemically prepared PEDOT/PSS (e-PEDOT/PSS) composites under various conditions. The comparative data provide valuable information about why there is so much difference between the ion transport properties of chemically prepared polymers and their electrochemically prepared counterparts.

5.2 RESULTS AND DISCUSSION

5.2.1 Preparation of PEDOT/PSS Composites

5.2.1.1 Electrochemical Methods

PEDOT/PSS composites were prepared from saturated 3,4-ethylenedioxythiophene (EDOT) aqueous solutions containing 0.1 M NaPSS by using a constant anodic current of 0.1 mA. A 0.072 cm^2 glassy carbon electrode was used as the working electrode. The reference electrode was a SSCE, and the counter electrode was a Pt wire. The potential during electrolysis changed from 0.9 V to 0.84 V vs SSCE.

PEDOT/PSS was also synthesized by cyclic voltammetry. Figure 5.1 shows representative cyclic voltammograms. The current increases evenly with increasing cycle number. This indicates the formation of electroactive PEDOT on the electrode, and also suggests that PEDOT/PSS is stable over the potential range of 0 V to +1 V.

Since the constant anodic current method has the advantage of ease of control of film thickness, it was chosen to synthesize polymers for the following study.

5.2.1.2 Chemical Methods

The c-PEDOT/PSS composites were prepared following a procedure reported by Lefebvre and coworkers [3]. That is by chemical oxidation of 100 mL of 0.05 M EDOT in $CH_3CN + H_2O$ (1:1) containing 0.05 M NaPSS with 50 mL of 0.69 M $Fe(NO_3)_3$(aq). After

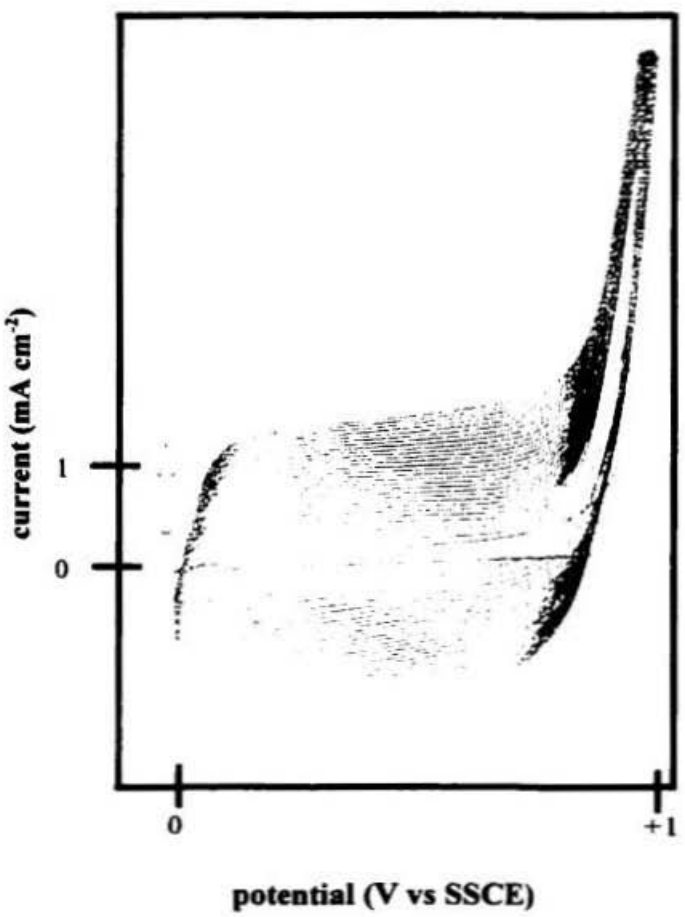

Figure 5.1. Cyclic voltammetric synthesis (100 mV s^{-1}) of PEDOT/PSS from a saturated aqueous EDOT solution containing 0.1 M PSS using a 0.071 cm^2 glassy carbon electrode.

24 hours of reaction at room temperature the black precipitate was collected by centrifugation, and it was dried under vacuum at room temperature. The PEDOT to PSS ratio of the composite is assumed to be ca.1.3 as reported by Lefebvre and coworkers [3].

5.2.2 Composition of the e-PEDOT/PSS Composites

The PEDOT to PSS ratio of one sample of e-PEDOT/PSS was determined by X-Ray emission analysis following complete reduction in 0.5 M KNO_3(aq). Since the K^+ content of the reduced film should be equal to its PSS content (Equation 5.2), the PEDOT to PSS ratio is given by n_{EDOT}/n_K, where n_K is the moles of K^+ incorporated into the sample, and n_{EDOT} is the moles of EDOT in the sample. PEDOT/PSS is completely reduced below the potential of -0.9 V vs SSCE in 0.5 M KNO_3(aq), as Figure 5.2 shows. Figure 5.3 shows EDX spectra of e-PEDOT/PSS films that had been reduced for 3 hours at 0 V and -1 V, respectively. They clearly show that K^+ ions have been incorporated into the polymer and that the molar ratio of K to S at -1 V is significantly higher than at 0 V. This is the expected result, since at 0 V PEDOT was only partly reduced and so less K^+ ions were incorporated (Equation 5.2). When the e-PEDOT/PSS was completely reduced, the molar ratio of K to S was 0.17, thus $n_K/(n_{PSS}+n_{EDOT}) = 0.17$, with an estimated 15% uncertainty. Since $n_K = n_{PSS}$, the PEDOT to PSS ratio of the polymer is ca. 4.8. That is five EDOTs sharing one PSS.

5.2.3 Thickness of e-PEDOT/PSS Films and c-PEDOT/PSS Layers

The thickness of a e-PEDOT/PSS film was determined with a micrometer by

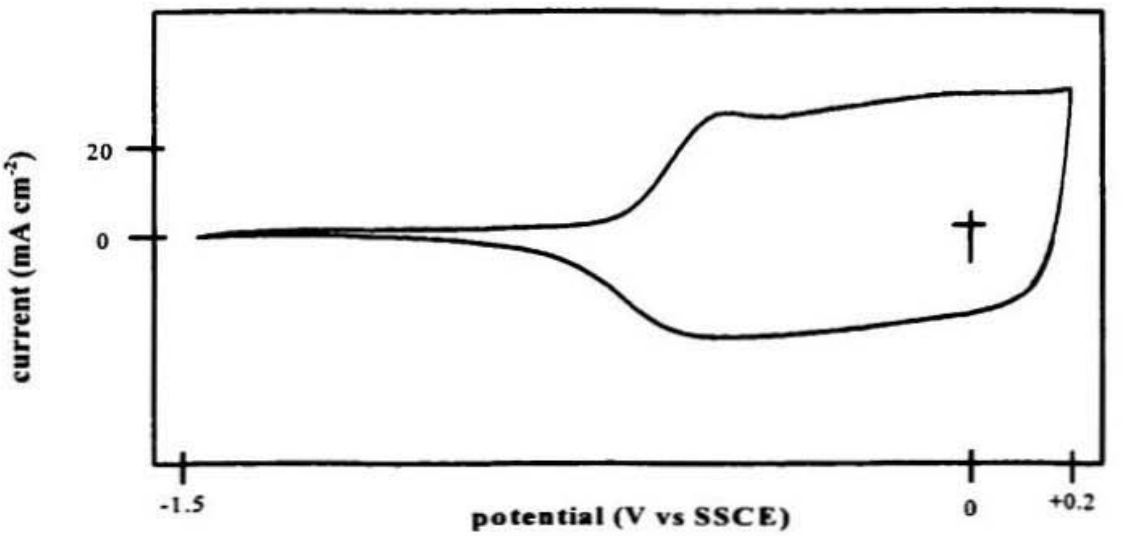

Figure 5.2. Cyclic voltammogram (40 mV s^{-1}) of a e-PEDOT/PSS film (19 μm) in 0.5 M KNO_3(aq).

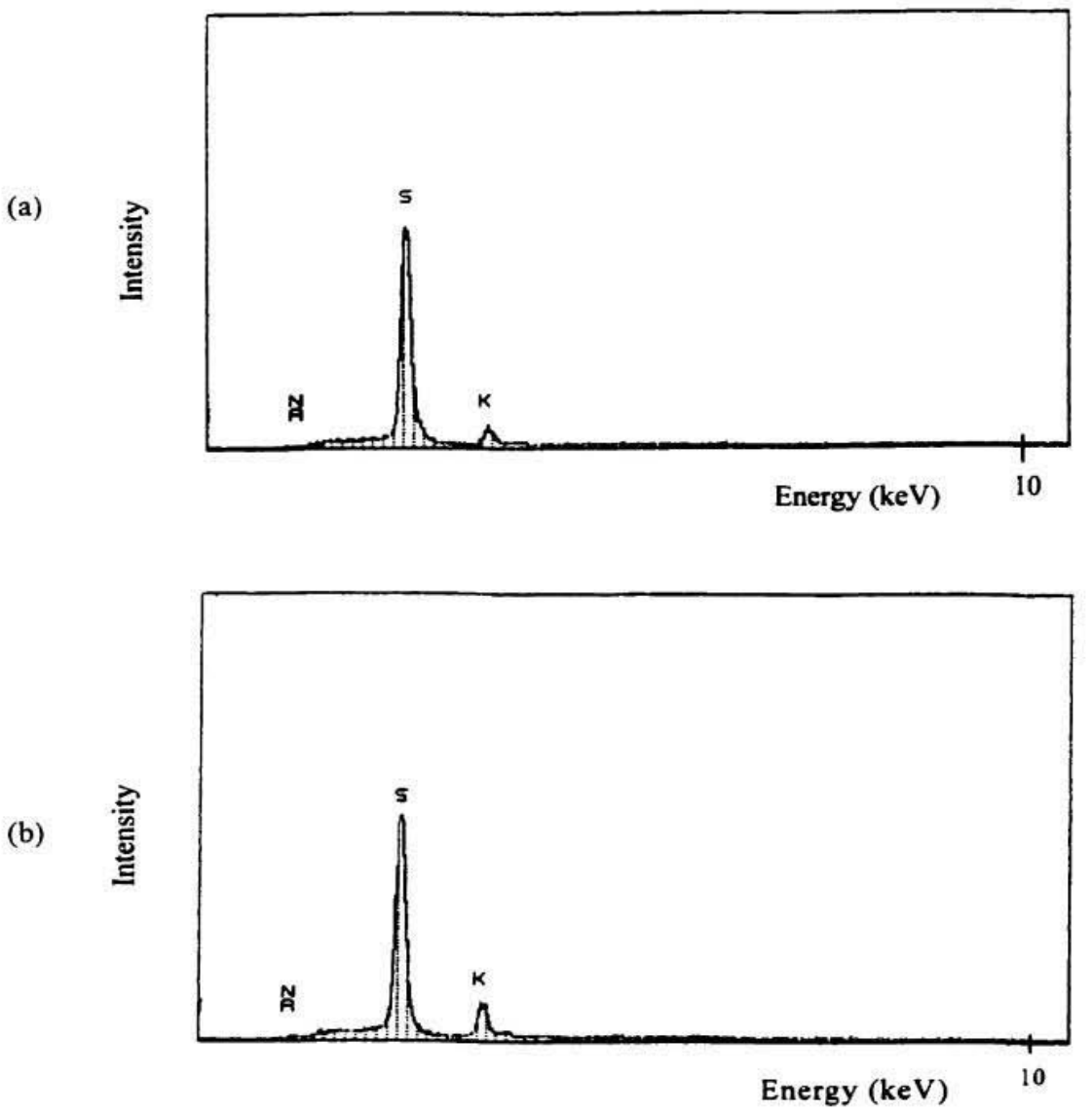

Figure 5.3. EDX spectra of a e-PEDOT/PSS film (19 μm) reduced in 0.5 M KNO_3 (aq) at (a) 0 V and (b) -1 V vs SSCE.

(a)

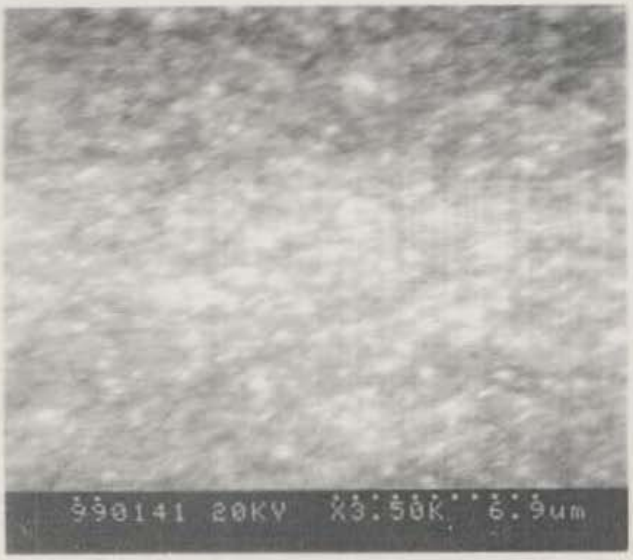

(b)

Figure 5.4. SEM micrographs of (a) e-PEDOT/PSS and (b) c-PEDOT/PSS.

measuring the difference in thickness of an ITO electrode (indium/tin oxide coated glass plate) before and after polymer deposition. The PEDOT/PSS film was deposited on the ITO from a saturated aqueous EDOT solution containing 0.1 M NaPSS. A constant anodic current of 0.4 mA was applied for 120 minutes. The area of the ITO immersed in the solution was 0.52 cm^2. The potential (vs SSCE) during electrolysis changed from 0.9 V to 0.82 V. The thickness of the polymer film was found to be 30 μm, yielding a relationship of 5.4 μm per 1C cm^{-2} of polymerization charge. The thickness of a c-PEDOT/PSS packed layer was measured with a micrometer. The thickness at a 2.5 mg cm^{-2} loading was 45 μm. Thicknesses of other films and layers were calculated based on these relationships.

5.2.4 Morphologies of e-PEDOT/PSS Films and c-PEDOT/PSS Powders

The morphologies of both e-PEDOT/PSS films and c-PEDOT/PSS powders were observed by scanning electron microscopy. The SEM micrographs (Figure 5.4) show that the e-PEDOT/PSS film is more compact than the c-PEDOT/PSS powder.

5.2.5 Cyclic Voltammetry

The electrochemical properties of the c-PEDOT/PSS composites were studied in various aqueous electrolyte solutions with the sandwich-type cell (Fig. 3.1), while the e-PEDOT/PSS composites were investigated in a conventional three-compartment cell. Cyclic voltammograms of both c-PEDOT/PSS and e-PEDOT/PSS in 0.5 M Et_4NCl(aq) are similar as Figure 5.5 shows, with large capacitance-like currents. The cyclic

voltammograms show only very small changes through multiple cycles over the potential range of -0.4 V to +0.4 V. This demonstrates the good stability of both c-PEDOT/PSS and e-PEDOT/PSS composites. Similar voltammetric properties were also observed in other aqueous electrolyte solutions (H_2SO_4, HCl, LiCl, $LiClO_4$, NaCl, $NaClO_4$, and Na_2SO_4) for both c-PEDOT/PSS and e-PEDOT/PSS composites.

Voltammetric currents increase almost linearly with increasing scan speed, even with the bulky Et_4N^+ counter-ions (Fig. 5.6). This indicates the facile electrochemistry of both c-PEDOT/PSS and e-PEDOT/PSS composites.

5.2.6 Impedance Spectroscopy

The ionic conductivities of both c-PEDOT/PSS packed layers and e-PEDOT/PSS films in various aqueous electrolyte solutions of H_2SO_4, HCl, $LiClO_4$, LiCl, NaCl, $NaClO_4$, Na_2SO_4, and Et_4NCl have been determined by impedance spectroscopy as a function of both concentration and applied potential.

Figure 5.7 shows complex plane impedance plots for a c-PEDOT/PSS packed layer and a e-PEDOT/PSS film, respectively. The general shape of these plots approximates the ideal behaviour [7] (almost 45° Warburg-like region and almost vertical low frequency region). The length of the Warburg-like region increases with decreasing concentration of the electrolyte. This indicates that the ionic resistances of both the c-PEDOT/PSS layer and e-PEDOT/PSS film increase with decreasing concentration of the electrolyte. Similar behaviour was also observed in other electrolyte solutions (Table 5.1 and Table 5.2). The

(a)

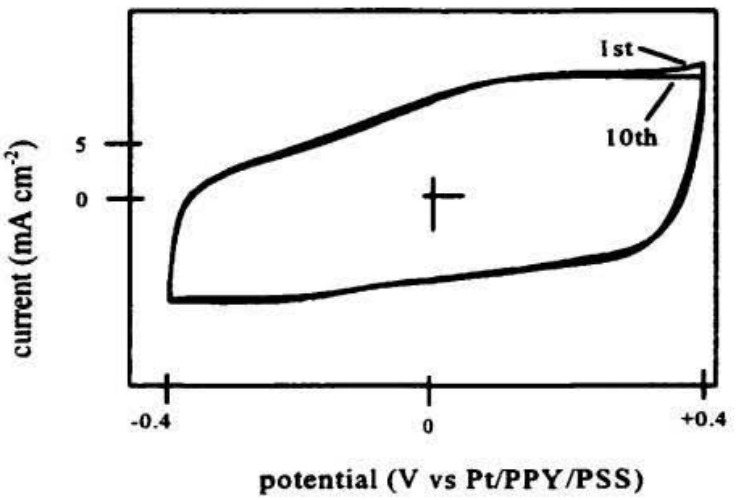

(b)

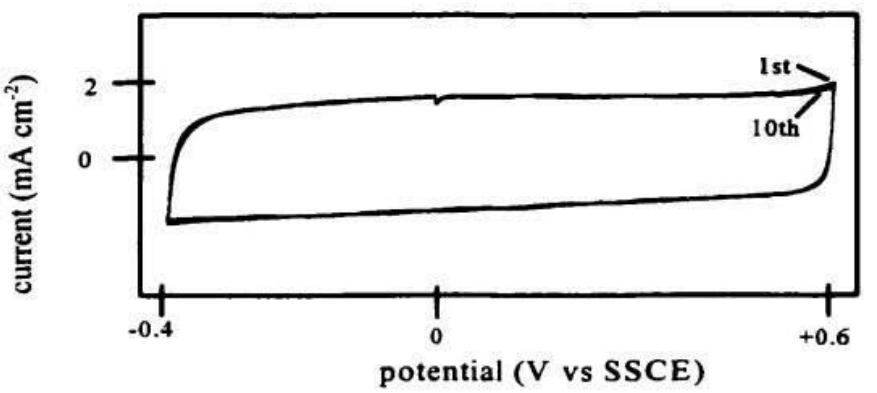

Figure 5.5. Cyclic voltammograms (20 mV s^{-1}) of (a) a c-PEDOT/PSS layer (5 mg cm^{-2}) and (b) a e-PEDOT/PSS film (14 μm) in contact with 0.5 M Et_4NCl(aq).

(a)

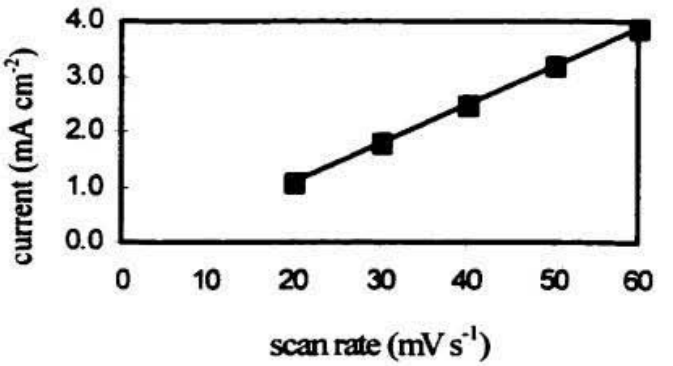

(b)

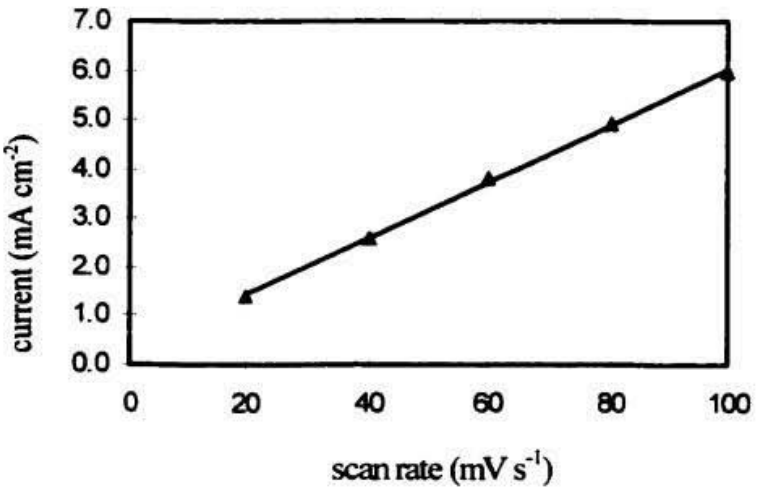

Figure 5.6. Anodic currents (at 0 V) of (a) a e-PEDOT/PSS film (14 μm) and (b) a c-PEDOT/PSS layer (2.5 mg cm^{-2}) as a function of scan rate in 0.5 M Et_4NCl(aq).

(a)

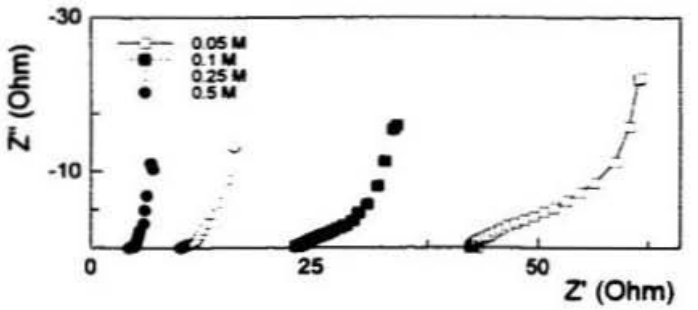

(b)

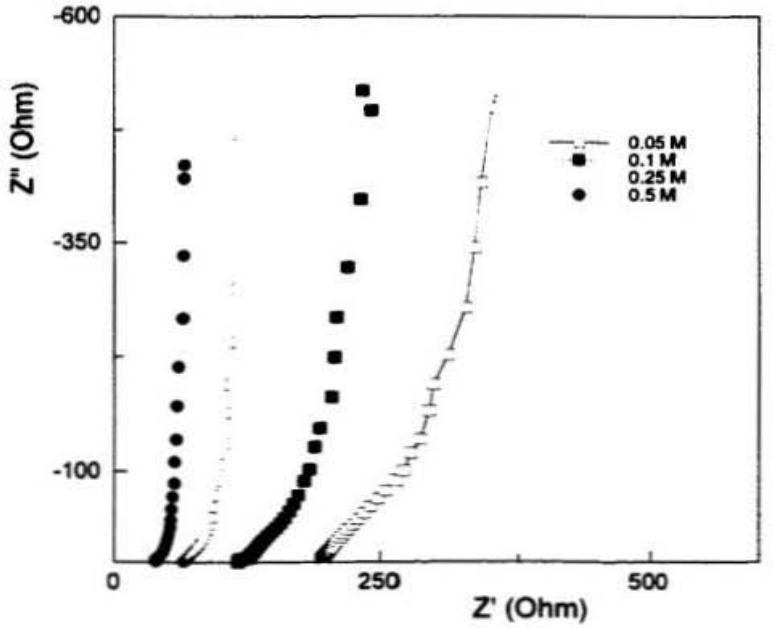

Figure 5.7. Complex plane impedance plots for (a) a c-PEDOT/PSS layer (2.5 mg cm^{-2}) at 0 V vs Pt/PPY/PSS and (b) a e-PEDOT/PSS film (14 μm) at 0.2 V vs SSCE in contact with LiCl(aq).

strong dependence of the ionic conductivity of the polymer on the electrolyte concentration shows that ion transport in both c-PEDOT/PSS and e-PEDOT/PSS composites is dominated by electrolyte in the pores [8].

Figures 5.8 and 5.9 show the ionic conductivities of c-PEDOT/PSS and e-PEDOT/PSS composites as a function of the conductivity of the electrolyte for various electrolytes and concentrations, with a linear least squares fit of all of the data. Again, these data show that the ionic conductivities of both c-PEDOT/PSS and e-PEDOT/PSS composites are dominated by electrolyte in pores. The y-intercepts of the linear least squares fit through all the data suggest that the intrinsic ionic conductivity of c-PEDOT/PSS is ca. 0.45 mS cm^{-1}, while the intrinsic ionic conductivity of e-PEDOT/PSS is too small to assess accurately from the data. The much higher intrinsic ionic conductivity of c-PEDOT/PSS than e-PEDOT/PSS is due presumably to the much higher content of PSS and Fe^{3+} ions in c-PEDOT/PSS. The Fe^{3+} ions are incorporated into the polymer to compensate the excessive PSS [3].

The slope of the linear regression in Figure 5.8 shows that the ionic conductivity of the c-PEDOT/PSS layer is ca. 27% of the solution conductivity. In contrast, the e-PEDOT/PSS film exhibits only ca. 2.5% of the bathing solution's conductivity. The conclusion from this comparison is that the c-PEDOT/PSS layer is about ten times more porous than the e-PEDOT/PSS film. This conclusion is supported by the scanning electron microscopy images (Figure 5.4).

The ionic conductivities of both c-PEDOT/PSS and e-PEDOT/PSS were found to

be independent of potential in high concentration electrolyte solutions (e.g. Fig. 5.10), indicating that ion transport is dominated by electrolyte in the pores [8]. However, in the low concentration solutions, there is a potential dependence as Figure 5.11 shows. The ionic conductivities increase with decreasing applied potential. This is the expected result since at lower potential more counter-ions are incorporated into the polymer (Equation 5.2). This result also indicates that the ionic conductivity of the polymer phase begins to become significant in low concentration electrolyte solutions.

The ionic conductivity of c-PEDOT/PSS shows much less potential dependence than that of e-PEDOT/PSS. This suggests that there is more electrolyte solution in the c-PEDOT/PSS layer, so c-PEDOT/PSS is more porous than e-PEDOT/PSS. This conclusion is supported by the scanning electron microscopy images (Fig. 5.4).

The ionic resistances of e-PEDOT/PSS films increase almost linearly with increasing film thickness, while the ionic conductivity is almost constant (Table 5.3).

Table 5.1. Ionic conductivities (mS cm^{-1}) of c-PEDOT/PSS layers in various aqueous electrolyte solutions at 0 V vs Pt/PPY/PSS.

Conc. (M)	H_2SO_4	HCl	$LiClO_4$	LiCl	$NaClO_4$	NaCl	Na_2SO_4	Et_4NCl
0.025	4.3							
0.05	7.3	6.1	1.0	0.48	3.7	3.9	2.2	1.1
0.1		14	2.1	1.4	5.1	4.6	5.7	2.1
0.125	#							
0.25	#	#	4.6	4.3	7.5	4.8	15	3.9
0.5		#	8.1	9.4	#	5.6	#	6.6

#: accurate data were not obtained due to very short Warburg-like regions and significant charge transfer resistances.

Table 5.2. Ionic conductivities (mS cm^{-1}) of e-PEDOT/PSS films in various aqueous electrolyte solutions at 0.2 V vs SSCE.

Conc. (M)	H_2SO_4	HCl	$LiClO_4$	LiCl	$NaClO_4$	NaCl	Na_2SO_4	Et_4NCl
0.025	0.57						0.17	
0.05	1.1	0.55	0.067	0.046	0.17	0.13	0.23	0.040
0.1		1.3	0.12	0.10	0.27	0.22		0.060
0.125	1.9						0.42	
0.25	3.3	2.4	0.21	0.18	0.52	0.39	0.55	0.079
0.5		3.5	0.31	0.27	0.94	0.67		0.14

Table 5.3. Ionic resistances and conductivities of e-PEDOT/PSS films in 0.5 M $LiClO_4$(aq) as a function of film thickness at 0.2 V vs SSCE.

Thickness (μm)	9.3	14	19	23
Ionic resistance (ohm)	42	56	73	107
Conductivity (mS cm^{-1})	0.31	0.35	0.37	0.30

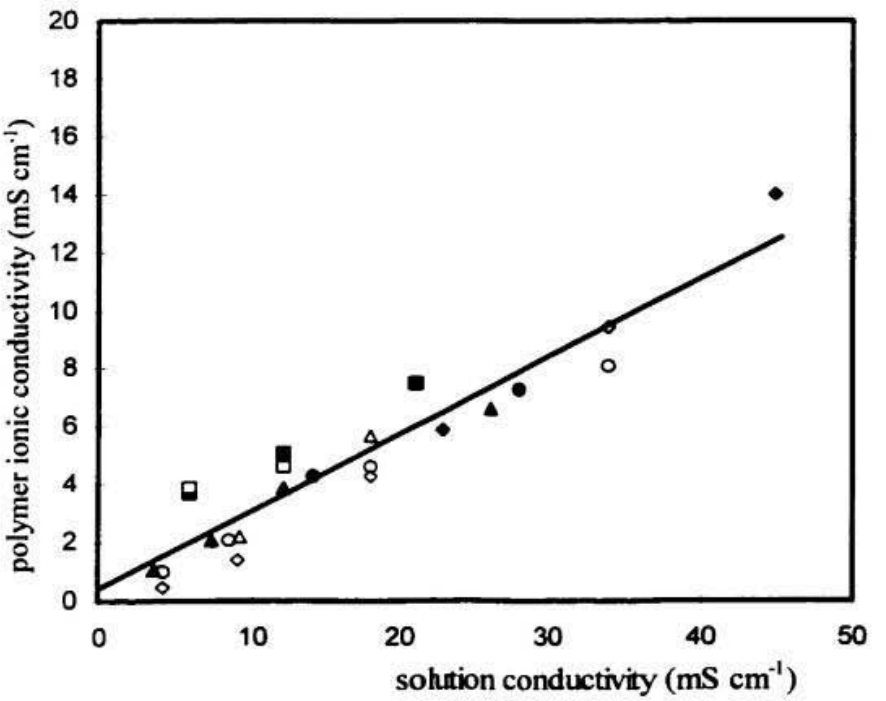

Figure 5.8. Ionic conductivity of c-PEDOT/PSS at 0 V vs Pt/PPY/PSS in aqueous solutions of H_2SO_4 (•), HCl (♦), $LiClO_4$ (○), LiCl (◇), $NaClO_4$ (■), NaCl (□), Na_2SO_4 (△), and Et_4NCl (▲), as a function of electrolyte conductivity. R^2 is ca. 0.89.

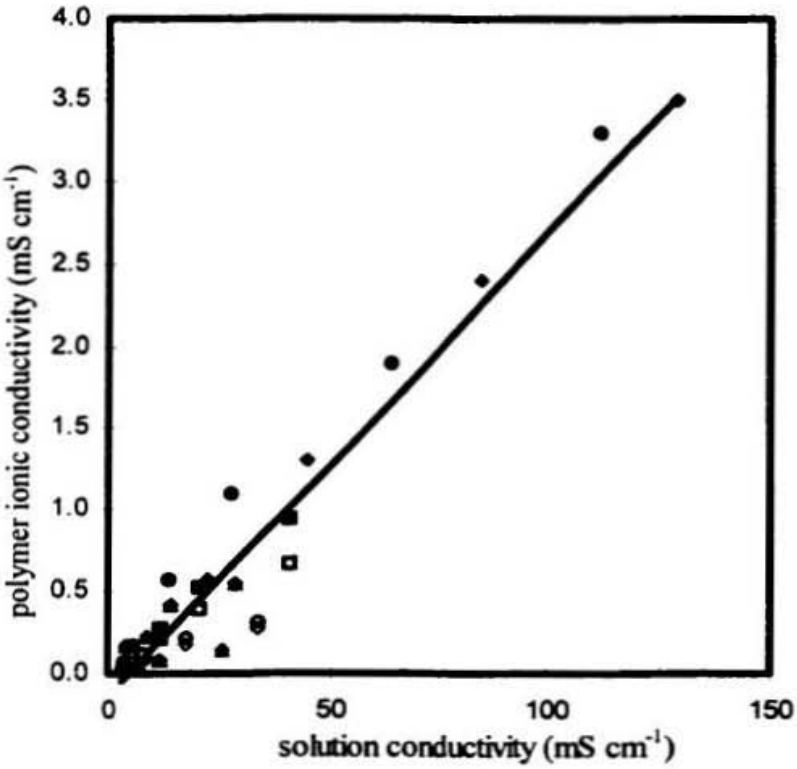

Figure 5.9. Ionic conductivity of e-PEDOT/PSS at 0.2 V vs SSCE in aqueous solutions of H_2SO_4 (•), HCl (♦), $LiClO_4$ (◦), LiCl (◇), $NaClO_4$ (■), NaCl (□), Na_2SO_4 (△), and Et_4NCl (▲), as a function of electrolyte conductivity. R^2 is ca. 0.92.

(a)

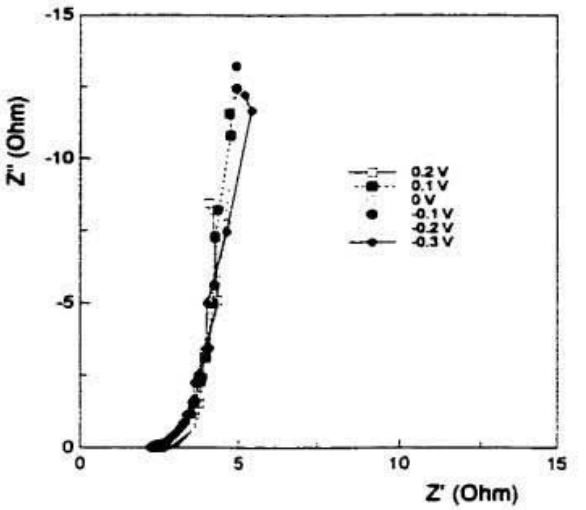

(b)

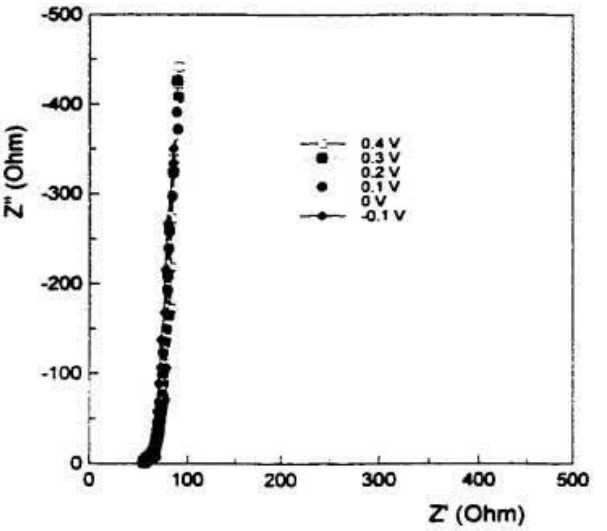

Figure 5.10. **Complex plane impedance plots for (a) a c-PEDOT/PSS layer (2.5 mg cm^{-2}) and (b) a e-PEDOT/PSS film (14 μm) in contact with 0.5 M $LiClO_4$(aq) at various applied potentials vs Pt/PPY/PSS for the c-PEDOT/PSS and SSCE for the e-PEDOT/PSS.**

(a)

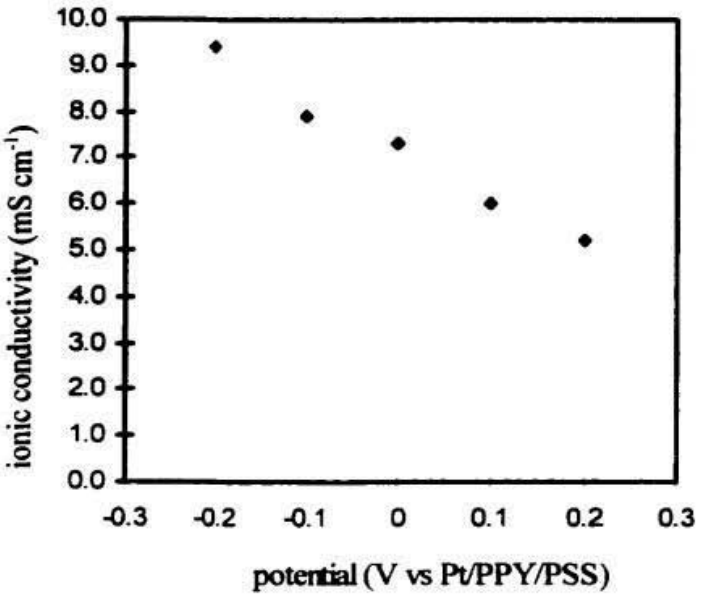

(b)

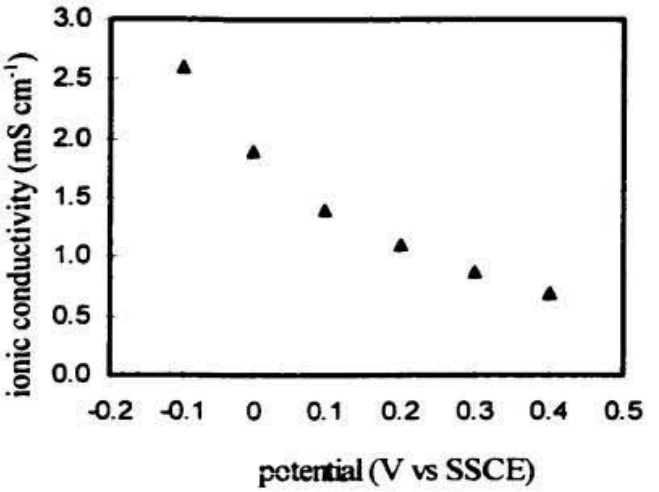

Figure 5.11. Ionic conductivities (mS cm^{-1}) of (a) c-PEDOT/PSS and (b) e-PEDOT/PSS in 0.05 M H_2SO_4(aq) as a function of applied potential.

5.3 CONCLUSIONS

PEDOT/PSS composites can be conveniently prepared from saturated aqueous EDOT solutions containing 0.1 M NaPSS. The ratio of PEDOT to PSS of c-PEDOT/PSS is significantly higher than that of e-PEDOT/PSS, and the intrinsic ionic conductivity of c-PEDOT/PSS is therefore much higher than that of e-PEDOT/PSS.

The electrochemistry of both c-PEDOT/PSS and e-PEDOT/PSS composites is facile. Ion transport in c-PEDOT/PSS packed layers is much faster than that in e-PEDOT/PSS films. The reason for this is that c-PEDOT/PSS is far more porous than e-PEDOT/PSS and therefore contains much more electrolyte solution.

The morphologies of both c-PEDOT/PSS and e-PEDOT/PSS can be represented by the model proposed for PPY/PSS (Fig. 4.15). That is, the polymer layer consists of permselective polymer aggregates (polymer phase) and pores containing electrolyte solution. In high concentration electrolyte solutions, ion transport is dominated by electrolyte solution in the pores, while in low concentration electrolyte solutions ion transport in the polymer phase becomes significant.

References

1. Winter, I.; Reese, C.; Hormes, J.; Heywang, G.; Jonas, F. *Chemical Physics* **1995**, 174, 207.

2. Carlberg, J. C.; Inganas, O. *J. Electrochem. Soc.* **1997**, 144, L61.

3. Lefebvre, M. C.; Qi, Z.; Rana, D.; Pickup, P. G. *Chem. Mater.* **1999**, 11, 262.

4. Gustafson, J. C.; Liedberg, B.; Inganas, O. *Solid State Ionics* **1994**, 145, 69.

5. Yamato, H.; Ohwa, M.; Wernet, W. *J. Electroanal. Chem.* **1995**, 397, 163.

6. Novak, P.; Muller, K.; Sonthanam, K. S. L.; Haas, O. *Chem. Rev.* **1997**, 97, 207.

7. Albory, W. J.; Mount, A. R. In *Electroactive Polymer Electrochemistry, Part 1: Fundamentals*; Lyons, M. E. G., Ed.; Plenum Press: New York, 1994; pp443-483.

8. Ren, X.; Pickup, P. G. *J. Electroanal. Chem.* **1995**, 396, 359.

Chapter 6 COMPARISON BETWEEN PEDOT/PSS AND PPY/PSS SYSTEMS AND GENERAL CONCLUSIONS

6.1 INTRODUCTION

Polypyrrole (PPY) is one of the most widely studied conducting polymers. Polypyrrole/poly(styrene-4-sulfonate) (PPY/PSS) composites have been found to have high electronic and ionic conductivity [1-2], and particularly high proton conductivity [3]. PPY/PSS has been investigated for many applications, such as batteries and fuel cells [4-5]. Poly(3,4-ethylenedioxythiophene) (PEDOT) is a relatively new conducting polymer. It has attracted increasing interest since it was first reported in 1992 [6]. PEDOT has been reported to exhibit high electronic conductivity, and, especially, higher chemical and electrochemical stability than PPY [7]. PEDOT/PSS has been exploited in a number of applications, such as fuel cells [5] and biosensors [8].

Both PPY/PSS and PEDOT/PSS composites can be conveniently prepared by electrochemical methods or by chemical oxidation. For electrochemical methods, both PPY /PSS and PEDOT/PSS can be easily prepared from aqueous solutions as thin films on electrodes; for chemical methods, a large amount of powder of PEDOT/PSS or PPY/PSS can be prepared rapidly.

6.2 COMPOSITION

The ratio of PPY to PSS of our chemically prepared sample was found to be ca. 5,

while the ratio of PEDOT to PSS of the chemically prepared sample was found to be ca 1.3 [9]. The PEDOT/PSS composite therefore has much higher content of PSS than does the PPY/PSS composite. The content of PSS in electrochemically prepared PEDOT/PSS (molar ratio) was found to be almost the same as that of electrochemically prepared PPY/PSS, that is about 20% of the composite.

6.3 ELECTROCHEMISTRY

Cyclic voltammograms of PPY/PSS and PEDOT/PSS are characteristic of conducting polymers, with large capacitance-like currents. Both PPY/PSS and PEDOT/PSS composites show facile electrochemistry, even in 0.05 M Et_4NCl aqueous solutions. They also show good electrochemical stability over the potential region of -0.6 V to + 0.4 V vs SSCE.

6.4 ION TRANSPORT

Ion transport in PEDOT/PSS was found to be much faster than in PPY/PSS (Table 4.5, 5.1, 5.2, and reference 2). Ionic conductivities of PEDOT/PSS in high concentration electrolyte solutions are about five times higher than those of PPY/PSS. Interestingly, the slope of polymer ionic conductivity as a function of solution conductivity for PEDOT/PSS is about five times higher than that of PPY/PSS. Since ion transport in high concentration electrolyte solutions is dominated by electrolyte in the pores, the clear conclusion from this comparison is that PEDOT/PSS is about five times more porous than PPY/PSS.

Another interesting finding is that ionic conductivities of chemically prepared

PEDOT/PSS and PPY/PSS are both about ten times higher than their electrochemically prepared counterparts.

The intrinsic ionic conductivity of chemically prepared PEDOT/PSS is about two and half times higher than that of chemically prepared PPY/PSS. This is presumably due to the higher content of PSS in PEDOT/PSS composites.

From standard deviation about the regression (Fig. 4.10, 5.8, and 5.9), relative errors in polymer conductivities can be estimated to be ca. 20% for c-PPY/PSS, 35% for e-PEDOT/PSS, and 22% for c-PEDOT/PSS. R^2 values are 0.91 for c-PPY/PSS, 0.89 for c-PEDOT/PSS, and 0.92 for e-PEDOT/PSS. The R^2 value of Fig. 4.9 is 0.99, which indicates the good reproducibility of ionic conductivity measurement for c-PPY/PSS.

6.5 MORPHOLOGY

Based on the ionic conductivity data and scanning electron microscopy images, PEDOT/PSS and PPY/PSS have similar morphologies, and both can be represented by a model proposed by Ren and Pickup [2]. That is, the polymers consist of permselective polymer phases and pores containing electrolyte solution.

Based on the ionic conductivity data, PPY/PSS is more compact than PEDOT/PSS, and, interestingly, chemically prepared PEDOT/PSS and PPY/PSS are both ten times more porous than their electrochemically prepared counterparts.

6.6 CONCLUSIONS

The ion transport data for PPY/PSS and PEDOT/PSS and scanning electron

microscopy images provide a clear picture of ion transport in conducting polymers and its dependence on morphology. That is, the polymers consist of permselective polymer phases containing incorporated counter-ions and pores containing electrolyte solution. Ion transport in a polymer is mainly dependent on electrolyte in the pores and incorporated ions in the polymer phases. The electrolyte in the pores accounts for the strong dependence of polymer ionic conductivity on solution concentration and conductivity, while the incorporated ions in the polymer phases are responsible for the potential dependence of polymer ionic conductivity and a polymer's intrinsic ionic conductivity.

In high concentration electrolyte solutions, ion transport in a polymer is dominated by electrolyte solution in the pores, while in low concentration electrolyte solutions, incorporated ions in the polymer phases become significant. The higher the concentration of incorporated ions in the polymer phases, the larger is the polymer's intrinsic ionic conductivity.

Two effective approaches can be taken to facilitate ion transport in a conducting polymer: one is to increase porosity of the polymer, and the other is to increase the content of incorporated counter-ions in the polymer phase.

The high electronic and ionic conductivities, facile electrochemistry, and ease of preparation give PEDOT/PSS and PPY/PSS composites great potential for use as energy storage materials. In particular, the cation exchange properties make them attractive to be used as cathodes in lithium ion batteries, and further work should be focused on the exploitation of PEDOT/PSS and PPY/PSS composites in this important application.

References

1. Qi, Z.; Pickup, P. G. *Chem. Mater.* **1997**, 9, 2934.

2. Ren, X.; Pickup, P. G. *J. Electroanal. Chem.* **1995**, 376, 357.

3. Qi, Z.; Lefebvre, M. C.; Pickup, P. G. *J. Electroanal. Chem.* **1998**, 459, 9.

4. Goffey, B.; Madsen, P. V.; Pochler, T. O.; Searson, P. C. *J. Electrochem. Soc.* **1995**, 142, 321.

5. Qi, Z.; Pickup, P. G. *Chem. Commun.* **1998**, 15.

6. Heywang, J. C.; Jonas, F. *Adv. Mater.* **1992**, 4, 116.

7. Carlberg, J. C.; Inganas, O. *J. Electrochem. Soc.* **1997**, 144, L61.

8. Yamato, H.; Ohwa, M.; Wernet, W. *J. Electroanal. Chem.* **1995**, 397, 163.

9. Lefebvre, M. C.; Qi, Z.; Rana, D.; Pickup, P. G. *Chem. Mater.* **1999**, 11, 262.